EBioMedicine 55 (2020) 102775

Contents lists available at ScienceDirect

EBioMedicine

journal homepage: www.elsevier.com/locate/ebiom

Research paper

Antimicrobial and antibiofilm activity of the EeCentrocin 1 derived peptide EC1-17KV *via* membrane disruption

Lingman Ma[a,1], Xinyue Ye[a,1], Pengbo Sun[a], Pengfei Xu[a], Liping Wang[a], Zixiang Liu[a], Xiaowei Huang[a], Zhaoshi Bai[b,*], Changlin Zhou[a,**]

[a] School of Life Science and Technology, China Pharmaceutical University, Nanjing, Jiangsu 211198, China
[b] Jiangsu Cancer Hospital & Jiangsu Institute of Cancer Research & the Affiliated Cancer Hospital of Nanjing Medical University, Nanjing, Jiangsu 210009, China

ARTICLE INFO

Article History:
Received 14 February 2020
Revised 1 April 2020
Accepted 15 April 2020
Available online xxx

Keywords:
Antibiotic resistance
AMP structural modification
EC1-17KV
Antimicrobial activity
Membrane destruction
Antibiofilm effect

ABSTRACT

Background: The antibiotic resistance and biofilm formation of pathogenic microbes exacerbate the difficulties of anti-infection therapy in the clinic. The structural modification of antimicrobial peptides (AMP) is an effective strategy to develop novel anti-infective agents.
Method: Seventeen amino acids (AA) in the longer chain of EeCentrocin 1 (from the edible sea-urchin Echinus esculentus) were truncated and underwent further modification. To produce lead peptides with low toxicity and high efficacy, the antimicrobial activity or cytotoxicity of peptides was evaluated against various multi-drug-resistant bacteria/fungi or mammalian cells *in vivo*/ *in vitro*. In addition, the stability and modes of action of the lead peptide were investigated.
Findings: EC1-17KV displayed potent activity and an expanded antimicrobial spectrum, especially against drug-resistant gram-negative bacteria and fungi, attributable to its enhanced amphiphilicity and net charge. In addition, it exhibits bactericidal/fungicidal activity and effectively increased the animal survival rate and mitigated the histopathological damage induced by multidrug-resistant *P. aeruginosa* or *C. albicans* in infected mice or *G. mellonella*. Moreover, EC1-17KV had a poor ability to induce resistance in bacteria and fungi and exhibited desirable high-salt/high-temperature tolerance properties. In bacteria, EC1-17KV promoted divalent cation release to damage bacterial membrane integrity. In fungi, it changed *C. albicans* membrane fluidity to increase membrane permeabilization or reduced hyphal formation to suppress biofilm formation.
Interpretation: EC1-17KV is a promising lead peptide for the development of antimicrobial agents against antibiotic resistant bacteria and fungi.
Funding: This work was funded by the National Natural Science Foundation of China (No. 81673483, 81803591); National Science and Technology Major Project Foundation of China (2019ZX09721001-004-005); National Key Research and Development Program of China (2018YFA0902000); "Double First-Class" University project (CPU2018GF/GY16); Natural Science Foundation of Jiangsu Province of China (No. BK20180563); and A Project Funded by the Priority Academic Program Development of Jiangsu Higher Education Institutions.

© 2020 The Author(s). Published by Elsevier B.V. This is an open access article under the CC BY-NC-ND license. (http://creativecommons.org/licenses/by-nc-nd/4.0/)

1. Introduction

The escalating crisis of multidrug resistance to antibiotics, associated with high morbidity and mortality, is raising fears of untreatable infections, and declining numbers of newly approved anti-infective agents worsen this situation [1]. Multidrug-resistant (MDR) strains of species such as *Enterococcus faecium*, *K. pneumoniae*, *P. aeruginosa* and *C. albicans* are largely responsible for such nosocomial infections, because they can aggregate and embed within a self-produced matrix of extracellular substances to form biofilms, which makes biofilm-based infections significantly less susceptible to antimicrobial agents than non-adherent or planktonic cells and thus extremely difficult to cure [2]. Currently, the therapeutic approach of MDR and extensively drug-resistant (XDR) *P. aeruginosa*, one of the main culprits for healthcare-related infections among gram-negative bacteria, is still

* Correspondence author: Jiangsu Cancer Hospital & Jiangsu Institute of Cancer Research & the Affiliated Cancer Hospital of Nanjing Medical University, Nanjing, Jiangsu 210009, China
** Correspondence author: School of Life Science and Technology, China Pharmaceutical University, 639 Longmian Avenue, Nanjing, Jiangsu 211198, China
E-mail addresses: baizhaoshi23@126.com (Z. Bai), cl_zhou@cpu.edu.cn (C. Zhou).
[1] These authors contributed equally to this work.

https://doi.org/10.1016/j.ebiom.2020.102775
2352-3964/© 2020 The Author(s). Published by Elsevier B.V. This is an open access article under the CC BY-NC-ND license. (http://creativecommons.org/licenses/by-nc-nd/4.0/)

controversial [3]. Additionally, antifungal drug resistance, especially to azoles, is prevalent in individuals with chronic mucocutaneous candidiasis [4]. However, the chronic use of amphotericin B or echinocandins in individuals who have azole resistance often induces toxicity (amphotericin B) or the emergence of resistance (echinocandins) [5]. Thus, the development of novel antimicrobial agents with different mechanisms, low toxicity, low drug tolerance and high efficacy seems necessary. Some antimicrobial peptides (AMP), which tend to form amphipathic structures, efficiently kill microbial pathogens by selectively interacting with microbial membranes *via* electrostatic interaction and then forming pores at the membrane surface to cause loss of membrane integrity. This results in relatively low chances of acquired resistance against AMP compared to other antibiotic classes [6-9]. Despite the early promise of AMP as alternatives to antibiotics, however, some problems, such as long sequences translating into high production costs, high haemolytic activity and cytotoxicity as well as susceptibility to *in vivo* enzymatic degradation and salt inactivation, limit the therapeutic applications [10]. Therefore, the design of synthetic AMP with short AA sequences, low toxicity and high efficacy and stability could be a promising strategy to improve the therapeutic applications of AMP in drug-resistant bacteria or fungi treatment.

Usually, to create a new generation of more potent and less toxic synthetic AMP congeners, we can obtain a wealth of sequence and structural information from the natural AMP originally isolated. EeCentrocin 1, a peptide isolated from *Echinus esculentus*, is intramolecularly connected *via* a disulfide bond to form a heterodimeric structure containing a cationic longer chain of 30 AA and a shorter chain of 13 AA. It exerts antibacterial activity against planktonic *C. glutamicum*, *S. aureus* and *P. aeruginosa*, mainly attributed to its longer chain [11]. However, the cysteine content and long peptide sequence of EeCentrocin 1 increase the cost and difficulty of synthesis. Moreover, the long chain of EeCentrocin 1 and the series of mutants derived from the longer chain all displayed relatively poor antifungal activity, as reported by Solstad et al [11, 12]. Although HC (1-12)A8K12 (P6), which has a highly ordered amphipathic structure with well-separated hydrophobic and cationic regions, exhibited potent antifungal activity, it showed 25% haemolysis at 200 μM [12]. In this study, we attempted to obtain a peptide with an expanded antimicrobial spectrum, lower cost and increased efficacy. Sometimes, the truncation combined to amino acid residue-selective substitution is a simple and effective method to obtain shorter derivatives with decreased toxicities and cost of production but increased activity, such as MCFA [13], HP-A3(A3-NT) [14], MSI-78 (4–20) [15], etc. In this study, the first 17 *N*-terminal AA residues, which have an abundance of hydrophobic and cationic residues and are important for the activity of small AMP [11, 16], were truncated from the longer chain of EeCentrocin 1 according to the results of computational prediction and was named EC1-17 (Fig. 1a). Although the sequence length of EC1-17 was greatly shortened, it exhibited no antimicrobial activity. The amphipathic structure consisting of a hydrophobic face that inserts between the lipid acyl chains of the membrane and a polar hydrophilic side that interacts with the lipid heads and the watery environment of the cytoplasm, is an important contributor to the antimicrobial action of small antimicrobial peptides [17, 18]. Lysine (Lys) and arginine (Arg), which have sufficient cationicity and can confer strong antimicrobial activities, are popular choices among the basic amino acids [10, 19]. In the EC1-17 sequence, we substituted Asp^8 with Lys, because the carboxyl chain of Asp^8 can counteract the positive charges of the structure. In addition, glycine, with the R group being a hydrogen atom, is known to be a more flexible residue and may lead to instability in the helical stretch [20, 21]. Thus, Gly^{14} was replaced by Val, a basic amino acid residue with suitable hydrophobicity and steric hindrance [22], producing EC1-17KV. This mutation might stabilize the peptide α-helix secondary structure and increase its amphiphilicity. Furthermore, Arg can form a higher number of electrostatic interactions than Lys and thus confers greater antimicrobial activities [10, 19]. Meanwhile, in our previous study, the Arg-rich peptide Cbf-14 has been confirmed to possess potent antifungal activity against *Cryptococcus neoformans* [23]. Therefore, in this study, all Lys in the sequence EC1-17KV were further replaced by arginine (Arg) to obtain EC1-17RV.

In this study, the antibacterial/antifungal spectrum of peptides designed against drug-sensitive or drug-resistant bacteria or fungi, especially MDR *P. aeruginosa* and fluconazole-resistant *C. albicans* was evaluated *in vivo/in vitro*. In addition, studies on structure-activity/structure-toxicity relationships and the underlying antimicrobial mechanisms were also investigated. This study will help in developing useful AMP and provide therapeutic strategies for infections caused by MDR *P. aeruginosa* and fluconazole-resistant *C. albicans*.

2. Materials and methods

2.1. Peptides and reagents

Peptides (purity>98%) were synthesized by GL Biochem (Shanghai, China). Other reagents were listed following: Penicillin V potassium, ceftazidime, polymyxin B, fluconazole, amphotericin B, gentamycin sulfate, ciprofloxacin monohydrochloride, Spin Column Yeast Total RNA Purification Kit (Sangon Biotech Co., Ltd, Shanghai, China); Mueller-Hinton broth (MHB), Columbia Blood Agar Base and Sabouraud's Glucose Agar/Broth Medium (Beijing SanYao Science & Technology Development Co., Beijing, China); TNF-α, IL-6, IL-1β and IL-18 ELISA Kits (Shanghai Meixuan Biological Science and Technology Ltd, Shanghai, China); Antibodies against NLRP3 (#15101), caspase-1 (#24232), cleaved caspase-1 (#89332), IL-1β (#31202), and cleaved-IL-1β (#52718) (Cell Signaling Technology, USA); HiFiScript 1st Strand cDNA Synthesis Kit and UltraSYBR Mixture (ComWin Biotech Co., Ltd, Jiangsu, China); 1-(4-(trimethylamino)phenyl)-6-phenylhexa-1,3,5-triene (TMA-DPH), DAPI, Propidium Iodide, FITC-ConA, SYPRO orange (Sigma, Taufkirchen, Germany); Cardiolipin (CL), Phosphatidyl cholines (PC), DPPG and DPPE (CordenPharma International, Plankstadt, Germany); LIVE/DEAD® BacLight™ Bacterial Viability Kit (ThermoFisher); Limulus Amebocyte Lysate Kit and E-TOXATE kits

a

EC1-17 GWWRRTVDKVRNAGRKV
EC1-17KV GWWRRTVKKVRNAVRKV
EC1-17RV GWWRRTVRRVRNAVRRV

Parameters	EC1-17	17KV	17RV
Molecular weight	2084.4	2139.6	2223.6
Net Charge	5	7	7
Hydrophobicity	0.079	0.138	0.134
μH	0.595	0.657	0.659
pI	10.05	12.48	13.78
GRAVY	-1.276	-1.029	-1.135
Aliphatic index	58.67	74.12	74.12

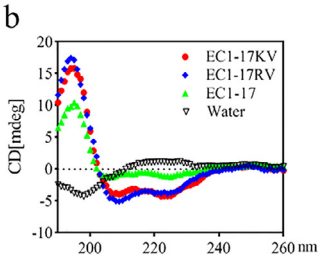

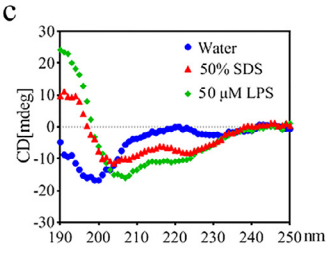

Fig. 1. Structure of the designed peptides. (a) Amino acid sequences and key physicochemical properties of different peptide mutants. μH: hydrophobic moment; GRAVY: grand average of hydropathy; pI: isoelectric point. (b) The conformation of peptides in 500 μM SUVs (DPPG/CL/DPPE at a mass ratio of 2:1:7) was analysed by circular dichroism. (c) CD assay for EC1-17KV secondary structure in different solutions.

(Xiamen Bioendo Technology, Co., Ltd., China); Calcium Ion Assay Kit and BCA Protein Assay Kit (Beyotime, Jiangsu, China). Other chemical reagents of analytical grade were purchased from commercial sources. The E-TOXATE kits were used to determine drugs. Test samples used in the study did not show detectable levels of endotoxin within the sensitivity limit of kit (0.1-1.0 EU/ml).

2.2. Bacterial strains and mammalian cells

Bacterial and fungal strains were purchased from the American Type Culture Collection (ATCC). All clinical strains were isolated from human clinical specimens by the Medical Laboratory Center of Zhongda Hospital (Nanjing, Jiangsu, China). Bacterial strains were prepared in MHB or Columbia Blood Agar Base and cultured at 37°C. Fungal strains were activated and passaged in Sabouraud's Glucose Agar/Broth Medium at 25°C. Raw 264.7, GES-1, human L02 and A549 cells were obtained from the Shanghai Institute of Cell Resource Center of Life Science (Shanghai, China) and cultured in DMEM or RPMI 1640 medium supplemented with 10% FBS at 37°C.

2.3. Planktonic activity assay

2.3.1. Detection of MIC and MBC/MFC

Planktonic test cells (1×10^5 CFU/ml) were added to medium containing two-fold serial dilutions of peptides or drugs, from 0.25 to 512 μg/ml. After 18 h of incubation at 37°C for bacteria or 72 h at 25°C for fungi, the minimum inhibitory concentration (MIC) was obtained by OD_{600}. The minimum bactericidal concentration (MBC) was determined after reading the MIC results; that is, a 10 μl mixture from the MIC was inoculated into Mueller-Hinton agar medium and subjected to 24 h of incubation and the first plate that observed bacterial growth was the MBC [24]. The method employed by the National Committee for Clinical Laboratory Standards was performed for minimal fungicidal concentration (MFC) detection [25]. To explore the effect of the divalent cation (Ca^{2+}) and metal-chelating agent EDTA on the antimicrobial activity of EC1-17KV, *P. aeruginosa* was suspended in Luria-Bertani containing different concentrations of $CaCl_2$ (0∼32 mM) or $CaCl_2$ (4.0 mM) + EDTA (0∼4.0 mM), and then mixed with the peptide for MIC value detection.

2.3.2. Disk diffusion assay

MDR *P. aeruginosa* or fluconazole-resistant *C. albicans* (100 μl) was evenly spread over Mueller-Hinton agar plates (with or without 2% glucose and 0.5 μg/ml beautyblue). Then, the disks containing EC1-17KV (20 μg), EC1-17RV (20 μg), polymyxin B (300 μg), ceftazidime (30 μg), fluconazole (20 μg), or amphotericin B (10 μg) were placed on the inoculated agar plates. After 24 or 72 h of culture, the inhibition zone diameter (IZD) of each disk was photographed and determined for the bacteriostatic activity assay.

2.3.3. Time-killing assay

The tested bacteria or fungi was respectively incubated with EC1-17KV, antibacterials or antifungal agents. Samples were shaken gently and aliquots were removed at the indicated time points for CFU counting by agar plate dilution method. Time-killing curves were constructed by plotting mean colony counts (log CFU/ml) *vs* time.

2.4. Antibiofilm activity assay

2.4.1. Biofilm and hyphal formation inhibition assay

C. albicans or *P. aeruginosa* (1×10^6 cells), suspended in RPMI 1640 medium or brain heart infusion supplemented with 2% glucose and 2 mM glutamine in the presence or absence of 16 μg/ml EC1-17KV, was inoculated into 96-well plates (poly-L-lysine- coated) and cultured at 37°C for 24 or 72 h. After the nonadherent cells were removed, crystal violet staining was employed to quantify biofilm at 595 nm. To observe hyphal formation, *C. albicans* suspension with or without EC1-17KV was inoculated into a 6-well plate (poly-L-lysine-coated) with glass coverslips and cultured at 37°C. At 1, 2, 4 and 8 h, the morphology and filamentation of *C. albicans* were observed. At 72 h, after removing the nonadherent *C. albicans*, the glass coverslips were stained by FDA for biofilm observation.

2.4.2. Biofilm dispersion ability detection

To investigate the effect of EC1-17KV on the mature biofilm, *P. aeruginosa* or *C. albicans* suspension was inoculated and cultured at 37°C for 24 or 72 h, with the corresponding medium change every 24 h. After gently washing off the nonadherent cells, fresh RPMI 1640 or BHI containing EC1-17KV was added for another 12 h of coincubation. Crystal violet staining and FDA staining were performed as described above to evaluate the antibiofilm activity of the peptide.

2.4.3. EPS reduction in preformed biofilms

Fluconazole-resistant *C. albicans* was seeded for biofilm formation. After washing, fresh YPD medium containing peptide (1 ×, 2 ×, 4 × MIC) was added for 24 h of incubation. Extracellular polymeric substance (EPS) components were then stained for 30 min at room temperature (carbohydrate: FITC-ConA, nucleic acids: DAPI, protein: SYPRO orange) after discarding the supernatant. The free dyes were washed, and the EPS components were observed.

2.5. Haemolytic activity and cytotoxicity

Sheep red blood cells (sRBCs) were washed with sterile saline until the supernatant was colorless. Cells suspension (3%) was incubated with serially diluted peptides for 1 h at 37°C. After centrifugation, the supernatant was collected for OD_{450} measurement. Cells incubated with 0.1% Triton X-100 was used as 100% haemolysis. The haemolysis percentage was calculated as previously described [26]. For cytotoxicity assay, cell lines (Raw 264.7, GES-1 and human L02) and spleen cells obtained from healthy mice with aseptic technique were suspended in medium to a density of 1×10^7 cells/ml, added with two-fold serially diluted peptides, from 16 to 1024 μg/ml, and incubated for 48 h. The routine MTT assay was performed and the IC_{50} (50% inhibiting concentration) of peptides towards different cells were calculated.

2.6. Circular dichroism

The conformation of EC1-17KV in 50% SDS, 50 μM LPS, 500 μM small unilamellar vesicles (SUVs, DPPG/CL/DPPE mass ratio system) or ddH_2O, and conformation of EC1-17 or EC1-17RV in 500 μM SUVs was analysed by circular dichroism (CD) at 37°C with a spectrum of 190-250 nm by a CD spectrophotometer (MOS 450) under scanning speed 100 nm/min, 0.1 cm quartz and a 1 nm bandwidth. Five scans were recorded for each sample.

2.7. Resistance study

Drug-susceptible *P. aeruginosa* or *C. albicans* was exposed to EC1-17KV, polymyxin B, ceftazidime, levofloxacin, fluconazole, or ketoconazole for MIC determination. After twenty-four similar serial passages exposing to the tested drugs (1/4 × MIC), the relative MIC was identified as the ratio of MIC obtained from the given subculture to that of first-time exposure.

2.8. Stability analysis

EC1-17KV solution was boiled for 10 or 30 min and then subjected to HPLC analysis or antibacterial testing to evaluate its high-temperature tolerance. For the high-salt tolerance test, EC1-17KV samples

coincubated with different concentrations of NaCl for 18 h were collected for HPLC analysis; meanwhile, *P. aeruginosa* treated with EC1-17KV containing NaCl for 18 h was used for the antibacterial test.

2.9. Antimicrobial activity assay in vivo

All experiments were performed in accordance with the Guidelines for the Care and Use of Laboratory Animals published by the US National Institutes of Health (NIH Publication No. 85-23, revised 1996) and approved by the Experimental Animal Ethics Committee of China Pharmaceutical University (2019-03-002).

2.9.1. Antibacterial activity of EC1-17KV in P. aeruginosa-infected systemic or local infection

Balb/c mice were purchased from the Laboratory Animal Center of Yangzhou University and housed in a temperature and light controlled environment. *In acute systemic infection,* MDR *P. aeruginosa* (1×10^9 CFU/ml) was intraperitoneally injected into mice (0.5 ml/mouse, n=16/group). Two hours later (early bacterial infection), mice were administered sterile saline, EC1-17KV (10, 5, 2.5 mg/kg) or polymyxin B (5.0 mg/kg). At 12 h postinfection, blood and lung samples from mice (n=6/group) were collected for CFU counting and ELISA. Additionally, lungs were homogenized for Western blot, ground in liquid nitrogen for qRT-PCR assay, or fixed with 4% polyformaldehyde for H&E staining. To assess the survival rate, ten remaining mice in each group were monitored daily for up to 7 days. *In subcutaneously implanted biofilm infection*, *P. aeruginosa* (1×10^8 CFU/mL) was inoculated into a 6-well plate and added with sterile catheter pieces (1 cm^2) for 24 h coincubation at 37°C to form biofilms. After washing off planktonic cells, the biofilm-containing catheter piece was implanted into the back skin of Balb/c mice, which have received three daily doses of cyclophosphamide (100 mg/kg of body weight, i.p, qd). Two days later, EC1-17KV (2.5, 5 or 10 mg/kg), PBS or polymyxin B (5 mg/kg) were injected into the subcutaneous tissue where the biofilm-containing catheter was implanted once daily for three continuous days. Twelve hours after the last administration, mouse skin tissue around the catheter was obtained for CFU counting and pathological examination (routine H&E staining). The catheter pieces were collected, centrifuged (12000 r/min, 10 min), mixed in a fast mixer for 10 min, and subjected to CFU counting.

2.9.2. Antifungal activity of EC1-17KV in C. albicans-induced G. mellonella infection

Final larval stage *G. mellonella*, weighing 200-250 mg, was inoculated with 10 μl fluconazole-resistant *C. albicans* (1×10^5 cells/larvae) *via* the last left proleg using a sterile microinjector. After 1 h postinfection, larvae (n=20/group) were injected with sterile saline, EC1-17KV (20, 10 and 5 μg) or fluconazole (10 μg) through the last right proleg (single injection of 10 μl) and then incubated at 37°C. Twenty-four hours later, when a large number of larvae began to die, the haemolymph was collected for the haemolymph melanization assay as described by Scorzoni *et al* [27] and the larvae were collected for CFU counting and H&E staining. Furthermore, larval survival and cocoon formation were monitored daily for up to 3 days. In the haemolymph melanization assay, the collected haemolymph was diluted to 1:10 in cold PBS, centrifuged for supernatant collection, and finally determined at 405 nm.

2.10. Inflammation detection

2.10.1. Elisa assay

Serum samples were collected and serum IL-6, IL-18, IL-1β and TNF-α were examined by ELISA kits according to the manufacturer's instructions.

2.10.2. Western blot

Lung homogenates in RIPA lysis buffer were quantified by BCA protein assay kit. Proteins were separated, transferred to polyvinylidene fluoride membrane, blocked, incubated with indicated primary antibodies (NLRP3, IL-1β, cleaved-IL-1β, caspase-1, cleaved caspase-1 and tubulin) and secondary antibody (goat anti-rabbit IgG HRP), and finally visualized using ECL reagents.

2.11. qRT-PCR assay

Total RNA from the lungs was extracted by TRIzol reagent. After reverse transcription to cDNA using the HiFiScript 1st Strand cDNA Synthesis Kit, PCR amplification was carried out using UltraSYBR Mixture. GAPDH served as the loading control. In addition, *C. albicans* was mixed with EC1-17 KV (16 μg/ml) or PBS for 8 h in RPMI 1640, and the pellets were collected for total RNA extraction using the Spin Column Yeast Total RNA Purification Kit. The reverse-transcribed cDNA was used as a template to amplify the hyphae-specific genes or ergosterol-related genes. 18S served as the loading control. All primers are listed in S1 Table.

2.12. Membrane disruption detection

2.12.1. NPN uptake and SYTO9/PI staining for membrane permeability

P. aeruginosa suspension (OD_{600} = 0.25) in 5 mM HEPES buffer (pH 7.4) was mixed with isovolumetric NPN solution (10 mM) dissolved in 95% ethanol. Thereafter, different concentrations of peptide were added. The real-time fluorescence of NPN was monitored at $\lambda_{ex/em}$ of 350/420 nm to determine EC1-17KV-induced outer membrane permeability [16]. In addition, *P. aeruginosa* suspension (1×10^6 CFU/ml) was incubated with EV1-17KV at 37°C for 2 h. The pellets were washed and resuspended in PBS, followed by the addition of the SYTO9/PI dye mixture. After 15 min of coincubation in the dark, bacteria were analysed by a flow cytometry to evaluate EC1-17KV-induced inner membrane permeability.

2.12.2. Calcein release assay

Calcein-loaded liposomes were prepared with DPPG/CL/DPPE or PC/cholesterol at a mass ratio of 2:1:7 or 10:1 to mimic the *P. aeruginosa* membrane or human erythrocyte cell membrane, respectively. Briefly, appropriate amounts of lipids were dissolved in chloroform. After vacuum evaporation and drying overnight, the lipid film was then hydrated at 60°C with a calcein solution (50 mM calcein, 50 mM TES, 100 mM NaCl, pH 7.4). Each mixture was ultrasonicated, repeatedly freeze-thawed, extruded, and washed off unencapsulated calcein as described in a previous study [28]. After obtaining the basal fluorescence of liposomes ($\lambda_{ex/em}$=490/530 nm), serially diluted peptide was added and 1% Triton X-100 was added as positive control. Fluorescence was measured at 0, 1, 5, 10, 15, 16 and 20 min after peptide addition. The calcein release rate was calculated as previously described [8]. In addition, the liposomes without calcein were also prepared by the film-dispersion method as described above to obtain SUVs [28].

2.12.3. TEM assay

P. aeruginosa or *C. albicans* (1×10^8 CFU/ml) was mixed with peptide (4 × MIC) for 3 or 6 h, respectively. Samples were centrifuged, mixed with 2% glutaraldehyde + 2% paraformaldehyde as a primary fixative (overnight at 4°C) and with 1% osmium tetroxide as a secondary fixative (1 h) after washing with PBS, subsequently dehydrated in an ethanol gradient (50, 70, 90% for 15 min each, 100% for 20 min), embedded in Epon 812, and finally double stained with 2% uranyl acetate (20 min) and lead citrate (5 min). The morphological change in bacteria or candida was observed using a JEM-1011 electron microscope (JEOL, Tokyo, Japan).

2.12.4. Detection of Ca^{2+} or K^+ concentration and bacterial LPS release

P. aeruginosa or *C. albicans* was centrifuged, washed and resuspended in PBS without Ca^{2+}/Mg^{2+} at density of 1×10^{10} CFU/ml, and then mixed with different concentrations of EC1-17KV at 37°C for 2 or 8 h. After centrifugation, the supernatant was collected and filtered through a 0.22 μm filter (Millipore, USA). The Ca^{2+} content in the supernatant was quantified using a Calcium Ion Assay Kit. LPS release was measured using a chromogenic limulus amebocyte lysate assay. The K^+ content in the supernatant from peptide-treated *C. albicans* was measured by an atomic absorption spectrometer (Varian, Palo Alto, CA, USA). In addition, to explore the effect of Ca^{2+} availability on LPS release, *P. aeruginosa* was suspended in PBS containing different concentrations of external Ca^{2+} (0∼1.0 mM) and added to EC1-17KV for 8 h of coincubation at 37°C. Finally, LPS release from *P. aeruginosa* in the presence of external Ca^{2+} was measured as described above.

2.12.5. C. albicans adhesion detection

Human buccal epithelial cells (HBECs) were obtained as described by Luanda *et al* [29] and mixed with *C. albicans* with MOI of 10. After the addition of EC1-17KV, the mixture was cultured at 37°C for 4 h with shaking (200 rpm). Cells were vortexed, formalin-fixed, vortexed again to remove nonadherent cells, and subjected to Wright staining to observe the adhesion of *C. albicans* to HBECs. In addition, *C. albicans* suspended in RPMI 1640 in the presence or absence of EC1-17KV was inoculated into a 96-well plate (poly-L-lysine-coated) for 2 h adhesion at 37°C. After discarding the supernatant and washing off free *C. albicans*, fresh RPMI 1640 was added for another 48 h culture. The XTT assay was performed to evaluate the adhesion rate of *C. albicans* with the following formula: (1-OD_{450} of samples/OD_{450} of control) × 100%. Moreover, *C. albicans* in RPMI 1640 was mixed with EC1-17KV (1, 2, 4 × MIC) and the pellets were collected after 24 h and resuspended to an OD_{600} of 1.0. Then, 2.0 ml of fungal suspension was mixed with 0.4 ml of xylene and the cell surface hydrophobicity (CSH) was detected and calculated as reported by Luanda *et al* [29].

2.12.6. The binding of EC1-17KV to C. albicans

The zeta potential on the surface of *C. albicans* in the absence or presence of different concentrations of EC1-17KV was detected by a ZetaPlus particle size analyser (Brookhaven Instruments Corporation, Holtsville,NY). In addition, *C. albicans* suspended in YEPD or RPMI 1640 medium was inoculated into a 6-well plate, cultured at 37°C for 2 h, and then mixed with FITC-labelled EC1-17KV (16 μg/ml) for another 30 min. After the unbound peptide was washed away, the binding activity of EC1-17KV to the surface of *C. albicans* (yeast and mycelial phase) was detected by flow cytometry and fluorescence microscopy, respectively.

2.12.7. Membrane fluidity analysis

To investigate whether EC1-17KV caused membrane instability, the membrane fluidity was determined using the fluorescent membrane probe TMA-DPH. *C. albicans* was treated with peptide for different time periods, incubated with TMA-DPH (1.0 μM) under low magnetic agitation for 10 min in the dark, and collected to determine the fluorescence polarization with $\lambda_{ex/em}$=350/452 nm as previously reported [30].

2.12.8. PI uptake and PI staining assay

C. albicans suspension was mixed with EC1-17KV solution (1 ×, 2 ×, 4 × MIC). After coincubation at 37°C for 4 h, *C. albicans* was washed with PBS and stained with PI solution (20 μg/ml) for flow cytometry assay and fluorescence microscopy detection.

2.13. Statistical analysis

Data were analysed by SPSS 22.0 software and presented as the mean ± SD. Comparison among groups was made by One-Way ANOVA Tukey Test of variance and Student *t*-test of unpaired data. P-value less than 0.05 was defined as significant differences.

3. Results

3.1. The structure and characterizations of the designed peptides

3.1.1. EC1-17KV has potent antimicrobial activity

The hydrophobicity and positive charges of the designed short peptides EC1-17KV and EC1-17RV were increased. As shown in Fig. 1a, both EC1-17KV and EC1-17RV have +7 charges, a greater hydrophobicity and aliphatic index than EC1-17. The CD analysis revealed a positive peak at 190 nm and two negative peaks near 208

Table 1
The MIC values of peptides (μg/ml (μM)).

	Strains	EC1-17	EC1-17KV	EC1-17RV	EeCentrocin 1	Penicillin V potassium	Ceftazidime	Fluconazole
G^+	*S. aureus* ATCC25923	>256 (>122.8)	32 (15.0)	256 (115.1)	16 (3.4)	2 (5.1)	1 (1.8)	-
	MRSA 1 [a]	>256 (>122.8)	64 (29.9)	256 (115.1)	16 (3.4)	>128 (>329.5)	>128 (>234.2)	-
	MRSA B9 [a]	>256 (>122.8)	32 (15.0)	128 (57.6)	16 (3.4)	>128 (>329.5)	64 (117.1)	-
	MRSA (EBSL+)	>256 (>122.8)	32 (15.0)	128 (57.6)	32 (6.9)	>128 (>329.5)	>128 (>234.2)	-
	S. epidermidis C6 [a]	>256 (>122.8)	64 (29.9)	256 (115.1)	64 (13.7)	>128 (>329.5)	>128 (>234.2)	-
	S. epidermidis C1 [a]	>256 (>122.8)	64 (29.9)	64 (28.8)	128 (27.5)	>128 (>329.5)	>128 (>234.2)	-
	Enterococcus faecalis [a]	>256 (>122.8)	16 (7.5)	32 (14.4)	16 (3.4)	>128 (>329.5)	>128 (>234.2)	-
	Mlicrococcus scarlatinae [a]	>256 (>122.8)	16 (7.5)	64 (28.8)	32 (6.9)	>128 (>329.5)	>128 (>234.2)	-
	S. pneumoniae [a]	>256 (>122.8)	128 (59.8)	128 (57.6)	64 (13.7)	>128 (>329.5)	>128 (>234.2)	-
G^-	*E. coli* ATCC25922	>256 (>122.8)	8 (3.7)	16 (7.2)	4 (0.9)	2 (5.1)	1 (1.8)	-
	E. coli A2 [a]	>256 (>122.8)	16 (7.5)	16 (7.2)	8 (1.7)	>128 (>329.5)	64 (117.1)	-
	P. aeruginosa CMCC10104	>256 (>122.8)	8 (3.7)	16 (7.2)	16 (3.4)	4 (10.3)	0.5 (0.9)	-
	P. aeruginosa ATCC27853	>256 (>122.8)	8 (3.7)	8 (3.6)	8 (1.7)	2 (5.1)	1 (1.8)	-
	P. aeruginosa 110 [a]	>256 (>122.8)	16 (7.5)	16 (7.2)	16 (3.4)	>128 (>329.5)	>128 (>234.2)	-
	P. aeruginosa 103 [a]	>256 (>122.8)	8 (3.7)	16 (7.2)	16 (3.4)	>128 (>329.5)	>128 (>234.2)	-
	K. pneumoniae ATCC10031	>256 (>122.8)	32 (15.0)	128 (57.6)	64 (13.7)	4 (10.3)	2 (3.7)	-
	K. pneumoniae [a]	>256 (>122.8)	64 (29.9)	128 (57.6)	128 (27.5)	>128 (>329.5)	>128 (>234.2)	-
Fungi	*C. albicans* ATCC10231	>256 (>122.8)	64 (29.9)	128 (57.6)	128 (27.5)	-	-	4 (13.1)
	C. albicans 7248 [a]	>256 (>122.8)	16 (7.5)	32 (14.4)	64 (13.7)	-	-	>128 (>417.9)
	C. albicans 006 [a]	>256 (>122.8)	8 (3.7)	16 (7.2)	32 (6.9)	-	-	4 (13.1)
	C. neoformans ATCC28957	>256 (>122.8)	16 (7.5)	32 (14.4)	128 (27.5)	-	-	2 (6.5)
	C. neoformans 4906 [a]	>256 (>122.8)	8 (3.7)	16 (7.2)	32 (6.9)	-	-	128 (417.9)
	C. neoformans 6120 [a]	>256 (>122.8)	16 (7.5)	32 (14.4)	64 (13.7)	-	-	>128 (>417.9)
	C. neoformans 001 [a]	>256 (>122.8)	8 (3.7)	32 (14.4)	32 (6.9)	-	-	2 (6.5)

[a] Clinical strains.

and 222 nm, representing alpha-helix: the peptides in 500 μM SUVs (a relevant membrane model) had α-helical content of 27.4% (EC1-17), 53.5% (EC1-17KV) and 57.3% (EC1-17RV), respectively; that is, EC1-17RV displayed a slightly higher α-helical content than that of EC1-17KV (Fig. 1b). Thus far, EC1-17 displayed no antimicrobial activity against all tested fungi and bacteria and negligible cytotoxic activity against mammalian cells which may be attributed to its low α-helicity and amphiphilicity. However, the substitution of Asp^8 and Gly^{14} with more electro-positive and hydrophobic amino acid residues significantly enhanced the antimicrobial activity and expanded the antimicrobial spectrum of the peptide. The results from the *in vitro* antimicrobial tests (Table 1) verified that the MIC of EC1-17KV against several clinical strains was 16∼64 μg/ml, especially against drug-resistant gram-negative bacteria and fungi including *P. aeruginosa*, *K. pneumoniae*, *C. albicans* and *C. neoformans*. Interestingly, the antifungal activity of both EC1-17KV and EC1-17RV was superior to that of EeCentrocin 1. Consistently, the bactericidal/fungicidal activity of EC1-17KV against MDR *P. aeruginosa* and *Enterococcus* and fluconazole-resistant *C. albicans* and *C. neoformans* was greater than that of the other tested peptides. Notably, after mutating the Lys in the sequence of EC1-17KV to Arg (in EC1-17RV), the activity of the peptide was decreased to some extent (Table 2). Furthermore, in the disk diffusion assay, EC1-17KV exhibited a stronger antimicrobial activity, with inhibition zone diameters (IZDs) of 4.5±0.2 mm or 5.6±0.3 mm against MDR *P. aeruginosa* or fluconazole-resistant *C. albicans*. However, the IZD of EC1-17RV was decreased to some extent (Fig. 2a). As verified in the haemolysis test, the haemolysis rate of SRBCs was less than 2% in samples treated with EC1-17KV or EC1-17 (512 μg/ml), which was 32-fold greater than the MIC value. In contrast, EC1-17RV-treated SRBCs displayed a slightly increased haemolysis rate, and the difference was significant at an EC1-17RV dose of 128 μg/ml ($p<0.05$, Fig. 2b, Fig. S1a). Consistently, the viability of mouse spleen cells in the EC1-17RV-treated group was lower than that in the EC1-17KV- or EC1-17- treated groups at the same dose (Fig. 2c, Fig. S1b). Similarly, the IC_{50} value of EC1-17KV or EC1-17 against mammalian cells was also higher than that of EC1-17RV (Fig. 2d, Fig. S1c). Herein, the effective antimicrobial concentrations of EC1-17KV were 8∼32 μg/ml, indicating that EC1-17KV could still be used as a safe antimicrobial agent. These results indicate that Arg replacement in EC1-17RV did not result in a more powerful antifungal peptide and that the increased Arg number may enhance the toxicity of helical AMP towards eukaryotic cells.

3.1.2. EC1-17KV circumvents the development of drug resistance

The resistance that could develop following multiple exposures of bacteria to EC1-17KV was assessed. As shown in Fig. 2e, after 24 subcultures following the initial exposure, the relative MIC of EC1-17KV against these two strains remained stable, suggesting no emergence of resistant bacteria. In contrast, against *P. aeruginosa*, the MICs increased by 4-fold for levofloxacin/ceftazidime and 16-fold for polymyxin B at the 8^{th} generation and increased by 16-fold for ceftazidime and 8-fold for levofloxacin at the 20^{th} generation. Against *C. albicans*, the MICs increased by 4-fold for fluconazole and ketoconazole at the 12^{th} generation and 8-fold for fluconazole at the 16^{th} generation, indicating that EC1-17KV can circumvent the development of drug resistance.

3.1.3. EC1-17KV displays desirable stability against high salt and high temperature

It has been reported that the antibacterial activities of some AMP are greatly attenuated by certain physical parameters, such as high salt and high temperature [31]. In this study, we found that the AA sequence and potent antimicrobial activity of EC1-17KV were not destroyed after boiling at 100°C for 10 and 30 min because the percentage of peptide remaining could still be maintained at 90.8 and 83.9, respectively. Furthermore, the activity of EC1-17KV was not affected by various concentrations of NaCl, showing that the percentage of peptide remaining was greater than 90 and that the MIC of this peptide against *P. aeruginosa* 110 was still 16 μg/ml when the NaCl concentration was increased from 100 to 400 mM, which is much higher than the human physiological salt concentration of 150 mM. These results indicate the high-salt and high-temperature resistance of EC1-17KV (Fig. 2f).

3.2. EC1-17KV exhibits bactericidal activity against drug-resistant pathogen in vitro

The bacterial or fungal killing activity of EC1-17KV was monitored by CFU counting after coincubation with peptide at dose of 4 × MIC, and compared with those of polymyxin B, ceftazidime, fluconazole, penicillin V potassium, vancomycin or amphotericin B, which are antibiotics in clinic with profound activities. As shown in Fig. 3a-b, for ceftazidime-resistant *E. coli* and *P. aeruginosa*, EC1-17KV could almost eliminate them within 4 h. Similarly, its bactericidal efficiency could also be observed in tested *E. faecalis* and *Mlicrococcus scarlatinae* (Fig. 3c-d), showing as the thorough elimination of bacteria within 8 h. Although EC1-17KV (64 μg/ml) exhibited a less pronounced effect than polymyxin B (32 μg/ml) or vancomycin (32 μg/ml) on killing tested bacteria, it significantly decreased the bacterial colonization within 2 h and no bacterial regrowth within 24 h was observed. This peptide also exerted potent killing effects on fluconazole-resistant *C. neoformans* and *C. albicans* as all fungi were eliminated within 8 h or 12 h (Fig. 3e-f), which were comparable with those of amphotericin B. It suggests that EC1-17KV has potent killing effects on drug-resistant bacteria and fungi.

3.3. EC1-17KV protects mice from bacterial infection

In a murine model of systemic infection, the intraperitoneal injection of MDR *P. aeruginosa* caused 80% and 100% mouse death on the 1st and 2nd days postinfection; however, EC1-17KV treatment significantly improved the animal survival rate in a dose-dependent manner, especially at a dose of 10 mg/kg EC1-17KV; at this dose, 90% of mice were protected from death. Furthermore, EC1-17KV was

Table 2
The MBC/MFC of peptides against drug-resistant bacteria and fungi (μg/ml).

	Strains	EC1-17	EC1-17KV	EC1-17RV	EeCentrocin 1	CAZ	Poly B	P-Vp	CFM	GTS	Vancomycin	FLU	AMB
G^+	*Enterococcus faecalis* [a]	>128	16	32	32	>128	-	>128	>128	>128	32	-	-
	Mlicrococcus scarlatinae [a]	>128	16	32	32	>128	-	>128	>128	>128	32	-	-
	P. aeruginosa 110 [a]	>128	16	16	64	>128	16	>128	>128	>128	-	-	-
G^-	*P. aeruginosa* 103 [a]	>128	16	8	32	>128	32	>128	>128	>128	-	-	-
Fungi	*C. albicans* 7248 [a]	>128	32	128	64	-	-	-			-	>128	8
	C. albicans 006 [a]	>128	32	32	32	-	-	-			-	16	8
	C. neoformans 6120 [a]	>128	16	32	128	-	-	-			-	>128	8
	C. neoformans 001 [a]	>128	16	16	64	-	-	-			-	8	4

CFM: Ciprofloxacin Monohydrochloride; GTS: Gentamycin Sulfate
[a] Clinical drug resistant strains. P-Vp: Penicillin V potassium; CAZ: Ceftazidime; Poly B: Polymyxin B; FLU: Fluconazole; AMB: Amphotericin B.

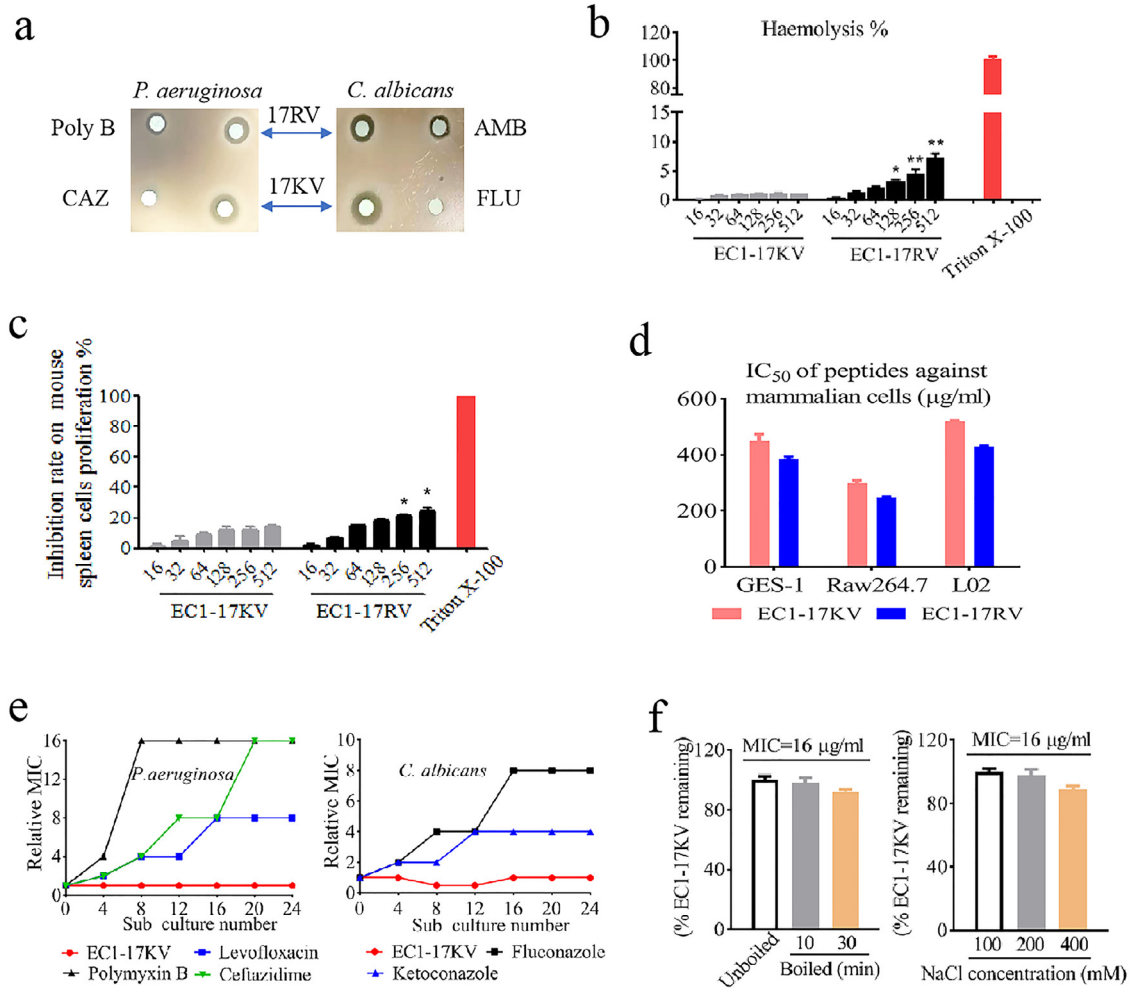

Fig. 2. Antimicrobial activity and toxicities of peptides. (a) Disk diffusion antibacterial assay. Poly B: polymyxin B; CAZ: ceftazidime; AMB: amphotericin B; FLU: fluconazole. (b) Haemolytic activity against SRBCs. 0.1% Triton X-100 is positive control, $^{*}p<0.05$; $^{**}p<0.01$ *vs* EC1-17RV at the same concentration [Student *t*-test]. The cytotoxicity of peptides to murine spleen cells (c) and other eukaryotic cells (d) was measured by MTT assay. (e) Drug resistance study for EC1-17KV in bacteria or fungi after 24 subcultures following the initial exposure. (f) The high-salt and high temperature tolerance of EC1-17KV was determined by HPLC and microdilution assays.

superior to polymyxin, the last line of defense against drug-resistant bacterial infections (Fig. 4a). This protective effect may be attributed to the significant reduction in bacterial counts in mouse lung and blood, approximate 5 or 2 log unit CFU reductions after 10 mg/kg EC1-17KV treatment (Fig. 4b).

The overproduction of proinflammatory cytokines, such as IL-1β, TNF-α and IL-6, are important predictors for the severity of bacterial infection [32]. However, peptides treatment, like HPA3P2, Cbf-14 and Fowl-1 (8-26)-WRK [8, 33, 34], alleviated inflammatory response induced by bacterial infection. Here, IL-1β, TNF-α, IL-6 and IL-18 contents in mouse serum were significantly increased after the intraperitoneal injection of *P. aeruginosa* for 12 h ($p<0.01$ *vs* the control group). Furthermore, the expression of these cytokines at the mRNA level in the mouse lungs showed a similar increase (Fig. 4c; Fig. S2). However, peptide treatment decreased secretion of these proinflammatory cytokines to some extent, and the difference in this inhibitory effect was significant when the peptide dose was greater than 5 mg/kg. This effect may be associated with the elimination of bacteria from mouse body. The release of IL-1β and IL-18 is mainly drove by caspase-1 processing which is facilitated by the NLRP3 inflammasome assembles in response to microbial invasion signals [35, 36]. The overactivation of the NLRP3 inflammasome results in the excessive release of IL-1β and IL-18; a continuous, uninterrupted and serious inflammatory response, and final lung injury aggravation. As evidenced by the western blot and ELISA, the dramatically increased expression and secretion of IL-1β and IL-18 by *P. aeruginosa* infection may be attributed to the overactivation of the NLRP3 inflammasome, reflected by the increased expression of IL-1β/cleaved IL-1β and caspase-1/cleaved caspase-1 (Fig. 4d). IL-1β, which is closely related to IL-6 and TNF-α, is recognized as an important contributor to the development of lung injury due to its potent inflammatory activity. In this study, a severe diffuse alveolar damage with intrapulmonary hemorrhage and edema accompanied by substantial inflammatory cell infiltration was observed in the lungs of *P. aeruginosa*-infected mice. In addition, the overproduction of IL-1β was also accompanied by the increased expression and secretion of IL-6 and TNF-α. As expected, following by the reduction in proinflammatory cytokine secretion, EC1-17KV treatment also led to a significant improvement in lung lesions, showing a gradual decrease in the scores of lung injury (the general indexes of pulmonary edema, congestion and inflammatory cell infiltration in the pulmonary interstitium and alveoli), as the peptide dose increased (Fig. 4e).

These observations demonstrate that EC1-17KV alleviates lung injury induced by MDR *P. aeruginosa* through inhibiting the systemic dissemination of bacteria to decrease the overactivation of the NLRP3

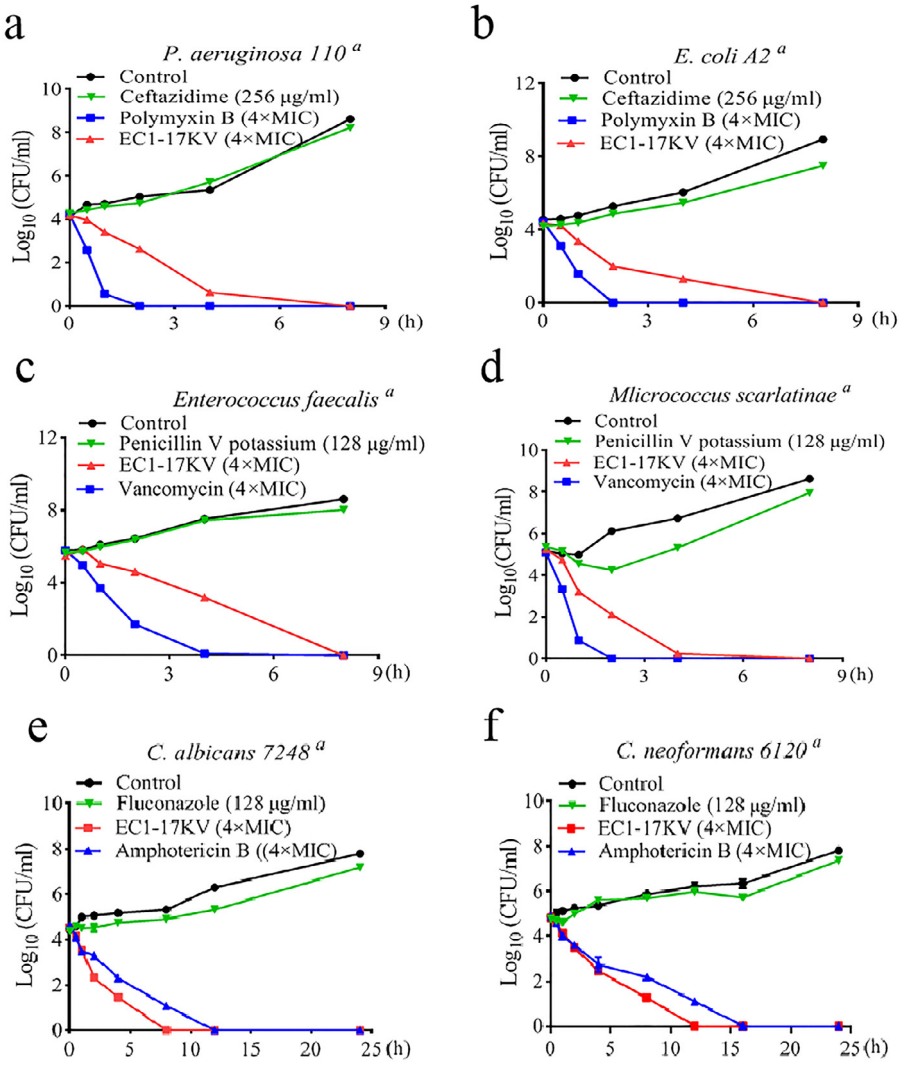

Fig. 3. Time-kill curves of EC1-17KV against drug-resistant bacteria or fungi. (a) MDR *P. aeruginosa*, (b) ceftazidime-resistant *E. coli*, (c) MDR *Enterococcus faecalis*, (d) MDR *Mlicrococcus scarlatinae*, (e) fluconazole-resistant *C. albicans*, (f) fluconazole-resistant *C. neoformans*. Control: treated with normal saline.

inflammasome and the excessive secretion of proinflammatory cytokines.

3.4. EC1-17KV damages bacterial membrane integrity by competitively replacing Ca^{2+} to bind to LPS

3.4.1. EC1-17KV disrupts the outer/inner membrane integrity of P. aeruginosa

NPN, a fluorescent probe, can be used to detect the integrity of bacterial outer membrane. Here, the outer membrane integrity of MDR *P. aeruginosa* was damaged by EC1-17KV in a time- and dose-dependent manner, because the fluorescence intensity gradually grew as the incubation time and drug concentration increased (Fig. 5a). In the SYTO/PI double-staining analysis, as the peptide concentration increased, the SYTO/PI (green/red) ratio decreased, indicating that the bacterial inner membrane integrity was compromised (Fig. 5b). The results from the TEM assay more intuitively revealed that after 2 h of coincubation with EC1-17KV (4 × MIC), the cell wall and membrane of *P. aeruginosa* were almost completely ruptured, showing obvious holes, leakage of intracellular contents and even the loss of the bacterial structure. In contrast, in the absence of the peptide, the bacteria presented a smooth surface, clearly visible structure and continuous double membrane (Fig. 5c). In addition, we also investigated whether bacterial membranes could be preferentially targeted by EC1-17KV. To this end, we evaluated the membrane perturbation by measuring calcein release from liposomes. As shown in Fig. 5d, the addition of EC1-17KV caused a rapid leakage of entrapped calcein from the negatively charged liposomes in a concentration- and time-dependent manner, especially at an EC1-17KV dose of 4 × MIC, which induced more than 80% leakage (green line in the right panel). However, this peptide was relatively ineffective at causing calcein release from uncharged PC/cholesterol liposomes, as only 7% leakage was observed after 15 min of exposure to 4 × MIC of the peptide (Fig. 5d, left panel).

3.4.2. EC1-17KV promotes the release of divalent cations and LPS

The replacement or chelation of divalent cations, which link the negatively charged phosphate groups between LPS molecules *via* ionic bridges, would disrupt bacterial membrane integrity [37]. In our study, EC1-17KV induced an obvious release of Ca^{2+} and LPS into the supernatant in a dose-dependent manner after 2 h of coincubation, and the difference was significant when the peptide dose reached 64 μg/ml (30 μM). This result suggests that EC1-17KV might competitively bind to LPS to release Ca^{2+} that originally form ionic bridges, resulting in the loss of Ca^{2+} from bacterial cell membrane and gradual destruction of bacterial membrane (Fig. 5e-f). Subsequently, external Ca^{2+} and/or EDTA was added to verify the mechanisms underlying the EC1-17KV-induced release of LPS and Ca^{2+}.

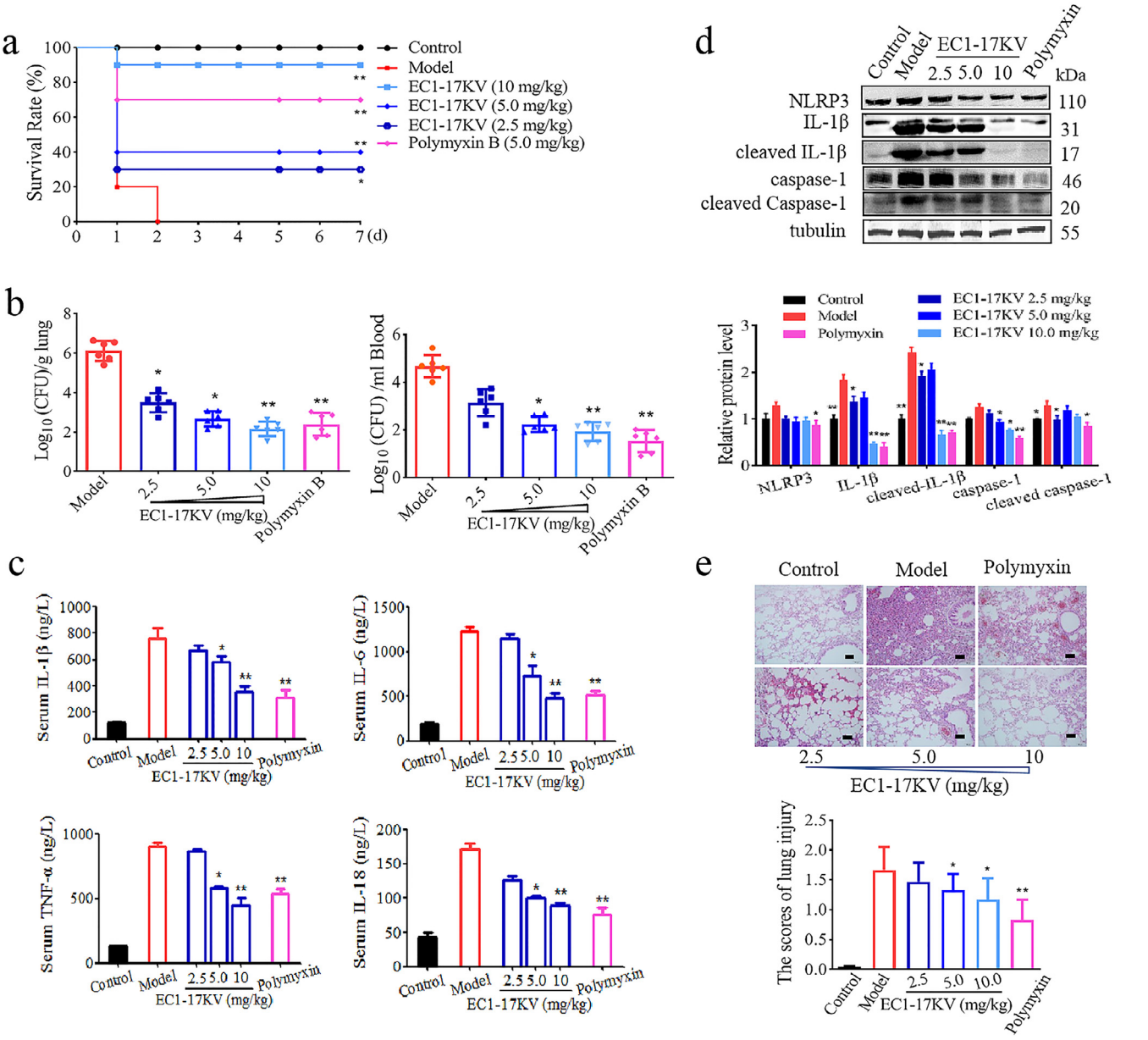

Fig. 4. EC1-17KV protects mice against MDR *P. aeruginosa*-induced acute systemic infection. (a) The survival rate of mice during the observation period of 7 consecutive days. (b) Bacterial counts in the lungs and blood of infected mice. (c) ELISA for the content of TNF-α, IL-6, IL-1β and IL-18 in mouse serum. (d) Western blot for the expression of NLRP3, IL-1β, cleaved IL-1β, caspase 1 and cleaved caspase-1 to measure the activation of the NLRP3 inflammasome. (e) H&E staining of mouse lungs. The total lung lesion scores were generated in a blinded manner by a certified pathologist according to a semi-quantitative scoring rank (right). Scale bars, 100 μm. $^{*}p<0.05$; $^{**}p<0.01$ *vs* model group [One-Way ANOVA Tukey test].

Interestingly, we found that EC1-17KV-induced LPS release from *P. aeruginosa* was significantly reduced as the concentrations of external Ca^{2+} increased, especially at Ca^{2+} concentrations greater than 0.5 mM (Fig. 5g). Importantly, in the presence of external Ca^{2+} ($\geq$1.0 mM), the MIC of EC1-17KV against *P. aeruginosa* were significantly increased (Fig. 5h). Moreover, we used the metal-chelating agent EDTA to chelate external Ca^{2+} (4.0 mM) and found that compared to EC1-17KV treatment alone, the chelation of the divalent cations decreased the MIC fold change from 1.0 to 0.0325 as the EDTA concentration increased from 0.125 to 4.0 mM (Fig. 5i), indicating that EC1-17KV may competitively replace the divalent cations from the bacterial membrane to exert its antibacterial effect.

3.5. EC1-17KV has potent antibiofilm activity against P. aeruginosa

In the biofilm formation assay, 12 strains of *P. aeruginosa* cultured in BHI medium supplemented with 2% glucose and 2 mM glutamine for 24 h formed mature biofilms. EC1-17KV (16 μg/ml) inhibited biofilm formation to some extent, especially against *P. aeruginosa* ATCC27853, *P. aeruginosa* 116, 110, 103, 114, 101 and 106, and the inhibitory effects were significantly greater than that of polymyxin B (Fig. 6a). Consistently, for the mature biofilm, this peptide also exhibited a desirable dispersion ability. That is, after 36 h of culture in a poly-L-lysine-coated 96-well plate, untreated *P. aeruginosa* formed a thick biofilm. However, EC1-17KV treatment significantly decreased the enhanced OD_{595} value (Fig. 6b). Furthermore, we implanted biofilm-containing catheter pieces into mouse back skin to evaluate the antibiofilm activity of EC1-17KV *in vivo* (Fig. S3). A large quantity of bacterial spread in subcutaneous tissue at five days postimplantation

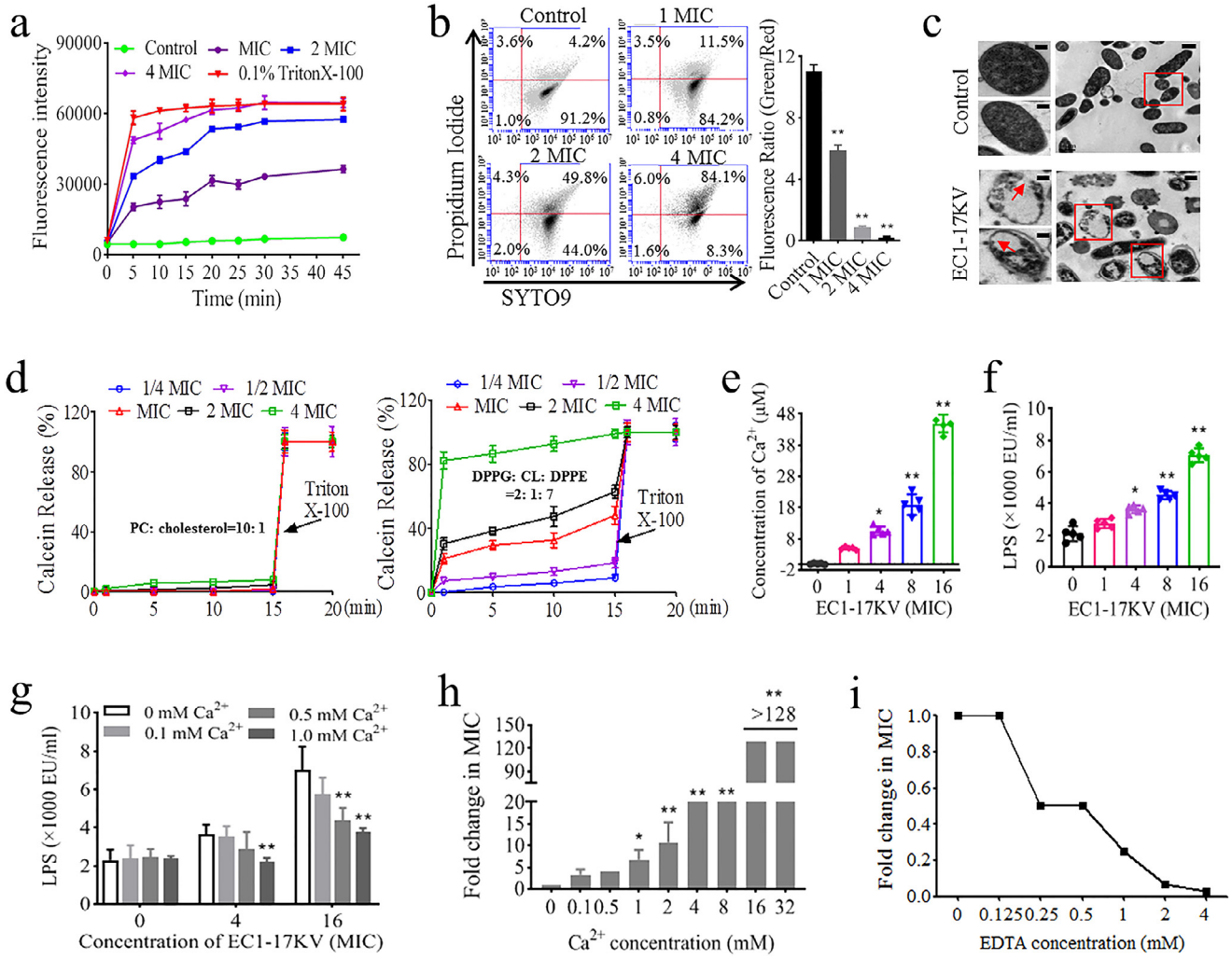

Fig. 5. EC1-17KV damages bacterial membrane integrity by competitively replacing Ca^{2+} to bind to LPS. (a) NPN uptake and (b) SYTO9/PI staining for outer and inner membrane permeability detection, the data are representative of three experiments. The increased fluorescence of NPN indicates increased outer membrane permeability, whereas a decreased SYTO (green)/PI (red) ratio means increased inner membrane permeability. (c) TEM assay of EC1-17KV-induced *P. aeruginosa* membrane disruption. Images in the dotted boxes are enlarged in the leftmost column. Red arrow: vacuoles or discontinuous cell membrane. (d) Leakage of entrapped calcein from EC1-17KV-treated liposomes. Left: artificial human erythrocyte cell membrane; Right: artificial *P. aeruginosa* membrane. (e) Ca^{2+} concentration and (f) LPS release in supernatant from peptide-treated *P. aeruginosa*. The effects of external Ca^{2+} on EC1-17KV-induced LPS release (g) and on the fold change of the peptide MIC (h). (i) The effect of EDTA on the fold change of the peptide MIC with external Ca^{2+} (4.0 mM). Scale bars: c (left): 200 nm; c (right): 1 μm. $^{**}p<0.01$ *vs* non-Ca^{2+} group [One-Way ANOVA Tukey test].

was observed, and this spread of *P. aeruginosa* caused severe edema, hyperemia and inflammatory cell infiltration. As expected, three days of treatment with EC1-17KV reduced the sessile bacteria attached on the catheter surface and inhibited the diffusion of bacteria from the catheter into the subcutaneous tissue in a dose-dependent manner (Fig. 6c). Thereafter, the peptide improved the inflammatory injury to the mouse subcutaneous tissue induced by the implanted-biofilm (Fig. 6d). Although 5 mg/kg EC1-17KV treatment displayed an obvious protective effect, high-dose EC1-17KV administration resulted in 3.5- and 2.7-log unit CFU reductions in the subcutaneous tissue and catheter surface, respectively, and produced the best protective effect against the inflammatory injury. Taken together, EC1-17KV has potent antibiofilm ability against MDR *P. aeruginosa*.

3.6. EC1-17KV protects G. mellonella against fluconazole-resistant C. albicans infection

In the sterile saline control group, 100% survival rate was observed; whereas in the model group, fluconazole-resistant *C. albicans* infection without drug treatment caused death in 100% of the larvae within 24 h. However, when the larvae were treated with EC1-17KV, the survival rate of *G. mellonella* increased to 50%, 70% and 80% in a dose-dependent manner (Fig. 7a). These survival rates were all higher than those of the 10 μg fluconazole-treated group (40% survival rate). In addition, as shown in Fig. 7b, counting *C. albicans* clones in the larval homogenates revealed that EC1-17KV significantly reduced the number of *C. albicans* clones, especially in the 10 or 20 μg EC1-17KV-treated groups where the reduction in *C. albicans* was greater than 2 log CFU. Fig. 7c-d shows cocoon formation and melanin production, which can be used to evaluate the vitality of *G. mellonella*. In the control group, full cocoon formation of all larvae was observed, and the cocoon seemed thick, corresponding to healthy larvae. However, in the model group, *C. albicans* infection caused *G. mellonella* death, and the larvae that died on the second day exhibited incomplete and thin cocoon formation. In addition, larvae from the model group had greater production of melanin than the control group. Because melanin aids can trap and kill pathogens, the production of melanin by *G. mellonella* occurs as a result of the immune response to the infection. Typically, the death of the larvae soon after correlated with complete melanization (a sign that the immune response being exhausted) in our study. Moreover, melanin production was also quantified by the optical density method, and

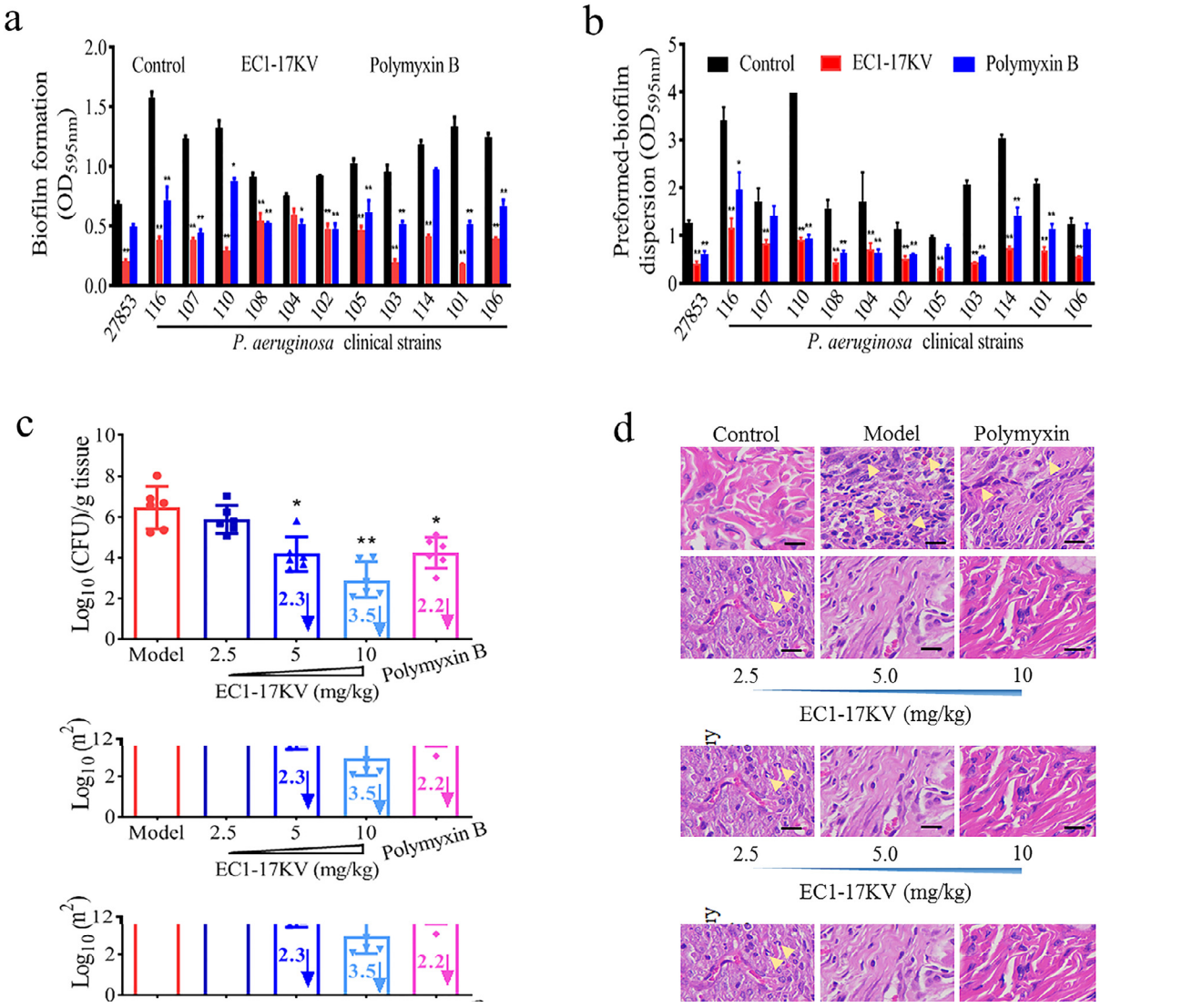

Fig. 6. EC1-17KV has potent antibiofilm activity against *P. aeruginosa*. (a) Biofilm formation or (b) preformed-biofilm dispersion in the presence or absence of EC1-17KV was measured by crystal violet staining. (c) Bacterial spread into the subcutaneous tissue or sessile bacteria attached to the catheter surface were counted by the plate dilution method. (d) H&E staining of mouse subcutaneous tissue infected by the implanted biofilm. Scale bars, 50 μm. $^{*}p<0.05$; $^{**}p<0.01$ *vs* model group [One-Way ANOVA Tukey test].

the result was consistent with the data above; the larvae in the model group had the highest level of melanin production. Importantly, consistent with the significant improvement in the larval survival rate, EC1-17KV treatment also improved the full cocoon formation and reduced melanin production, as evidenced by the complete and thick cocoon formation and lack of melanin production in the surviving larvae. In addition, results from H&E staining indicated that the tissue injury induced by *C. albicans* infection could also be alleviated by EC1-17KV, reflecting as the mitigated tissue hyperemia and inflammatory cell infiltration (Fig. 7e). By contrast, fluconazole exhibited a weaker protective effect on drug-resistant *C. albicans*-infected *G. mellonella* than EC1-17KV at the same dose or even a lower dose, indicating that EC1-17KV protects *G. mellonella* against fluconazole-resistant *C. albicans* infection.

3.7. EC1-17KV exerts fungicidal effects by disrupting fungal membrane integrity

A considerable number of previous researches report that the disruption of the cellular membrane integrity resulting in the leakage of ions and other molecules is believed to be the major mode of action for cationic AMP against fungi [38].

3.7.1. EC1-17KV binds to the C. albicans surface

As evidenced by the zeta potential assay, the *C. albicans* surface was negatively charged (-31.1 mV) and EC1-17KV dose-dependently neutralized the negative charges (from -31.1 to -0.37 mV, Fig. 8a). Subsequently, EC1-17KV aggregated on the surface of *Candida* in both yeast and mycelial forms because the fluorescence intensity gradually increased as the peptide concentrations increased over 30 min (Fig. 8b). Furthermore, a large number of FITC-EC1-17KV-labelled *C. albicans* cells were observed by fluorescence microscopy (Fig. 8c). Interestingly, the amount of FITC-EC1-17KV aggregated on the surface of the mycelial phase was greater than that of the yeast phase, especially at EC1-17KV concentrations greater than 2 × MIC.

3.7.2. EC1-17KV disrupts fungal membrane integrity

Subsequently, direct morphological changes in the *C. albicans* membrane were observed by TEM. As shown in Fig. 8d, in addition to a smooth and continuous double-membrane structure, a ribosome-

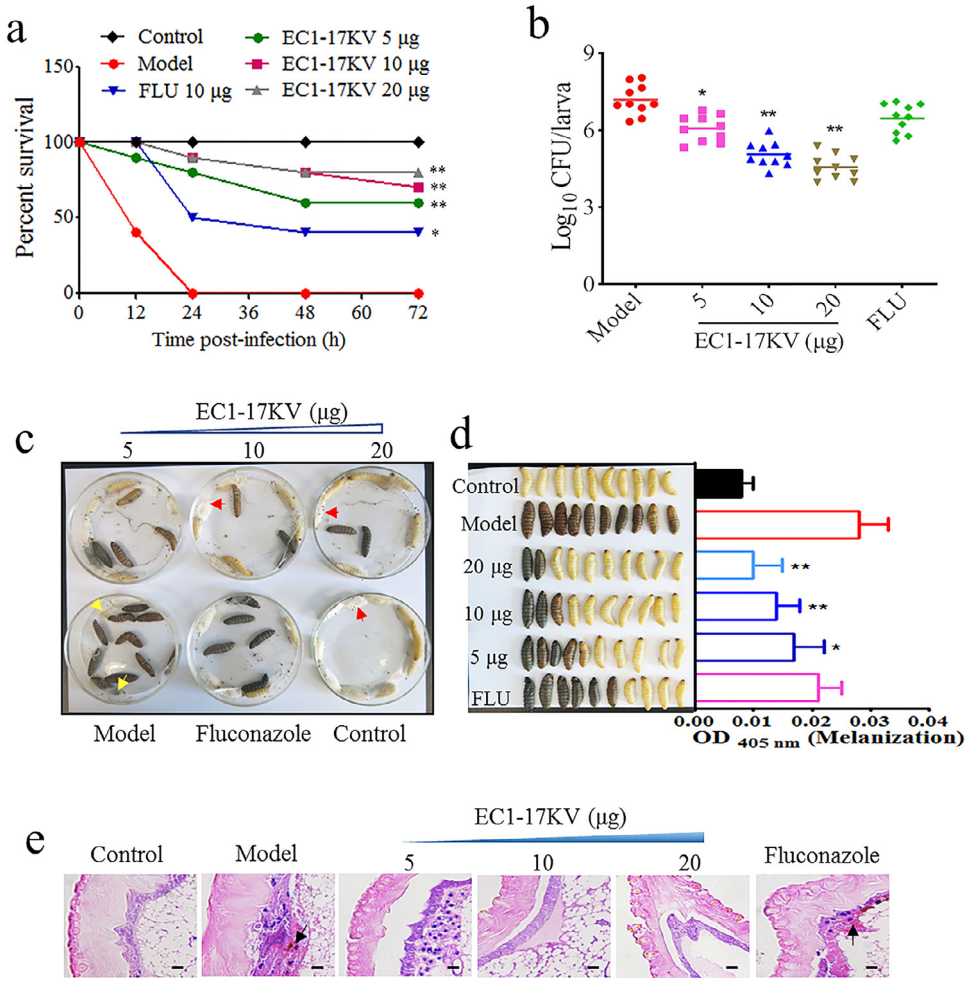

Fig. 7. Effective antifungal activity of EC1-17KV in *C. albicans*-infected *G. mellonella*. (a) Survival plot of *G. mellonella* after inoculation with *C. albicans* and treatment with a single dose of EC1-17KV or fluconazole over 72 h postinfection. (b) Plate dilution method for CFU counting in the larval homogenate after 24 h of infection. (c) Visual appearance of larvae and cocoon formation of *G. mellonella*. Red arrow: complete and thick cocoon; yellow arrow: incomplete and thin cocoon. (d) Melanization of *G. mellonella* after *C. albicans* injection was measured by the optical density (OD) of the haemolymph. (e) H&E staining of larvae in the presence or absence of EC1-17KV treatment. Black arrow: hyperemia and inflammatory cell infiltration; Control: non-infected larvae; Model: infected larvae with saline treatment; FLU: 10 μg fluconazole. Scale bars, 100 μm. $^{*}p<0.05$; $^{**}p<0.01$ *vs* model group [One-Way ANOVA Tukey test].

rich cytoplasm surrounding the DNA-containing nucleus was observed in untreated fungi. In contrast, EC1-17KV (4 × MIC) treatment produced uneven cytoplasmic content distribution and noticeable disruption of the plasma membrane and intracellular organelles. The structure of the nuclei was difficult to identify, with the nuclear membrane being either missing or fully degraded. Furthermore, the results of the PI staining and PI uptake tests all demonstrated that at EC1-17KV concentrations greater than 2 × MIC, PI dye uptake by DNA was increased, indicating that EC1-17KV disrupts fungal membrane integrity (Fig. 8e-f). The results from K^+ release test showed that K^+ content increased in the culture medium of *C. albicans* exposed to EC1-17KV as the peptide dose increased. At the MIC concentration (16 μg/ml), 31.5% leakage of K^+ was observed; however, the leakage rate was greater than 77.9% after 8 h of incubation at peptide concentrations up to 4 × MIC, suggesting an increase in cell membrane permeability (Fig. 8g). To study why EC1-17KV could induce fungal cell membrane permeabilization, the expression changes of ergosterol synthesis-related genes, including *ERG1*, *ERG7*, *ERG27* and *ERG28*, were measured. However, the peptide had no influence on the expression of ergosterol synthesis-related genes, see Fig. 8h. Thereafter, the change in cell membrane fluidity in the presence of EC1-17KV was detected by TMA-DPH. The results demonstrated that the relative fluorescence intensity of DPH dye decreased from 100% to 70.0% as the peptide concentration increased from 0 to 64 μg/ml (Fig. 8i) after 120 min of coincubation, which was similar to that of Amphotericin B. This suggests that EC1-17KV may insert into the lipid bilayer of the *C. albicans* cell membrane because the polarization of TMA-DPH reflects perturbations in the hydrophobic region of the lipid bilayer, whereas the membrane fluidity and fluorescence polarization are inversely correlated [39].

3.8. EC1-17KV exerts antifungal activity by inhibiting hypha and biofilm formation

Majority of *C. albicans* infections are associated with biofilm formation on host or abiotic surfaces. *C. albicans* virulence depends on its ability to adhere and form biofilms on many surfaces [40].

3.8.1. EC1-17KV reduces the adhesion of C. albicans

Here, the effect of EC1-17KV on *C. albicans* adherence to HBECs or the surface of a cell culture plate as determined by Wright staining and the XTT method. As shown in Fig. 9a, after exposure to different concentrations of EC1-17KV, the number of fungi adhering to HBECs decreased in a dose-dependent manner. There were a few countable and short hyphae adhered to the HBEC surface at EC1-17KV concentrations up to 16 or 64 μg/ml. Consistently, the results from the XTT

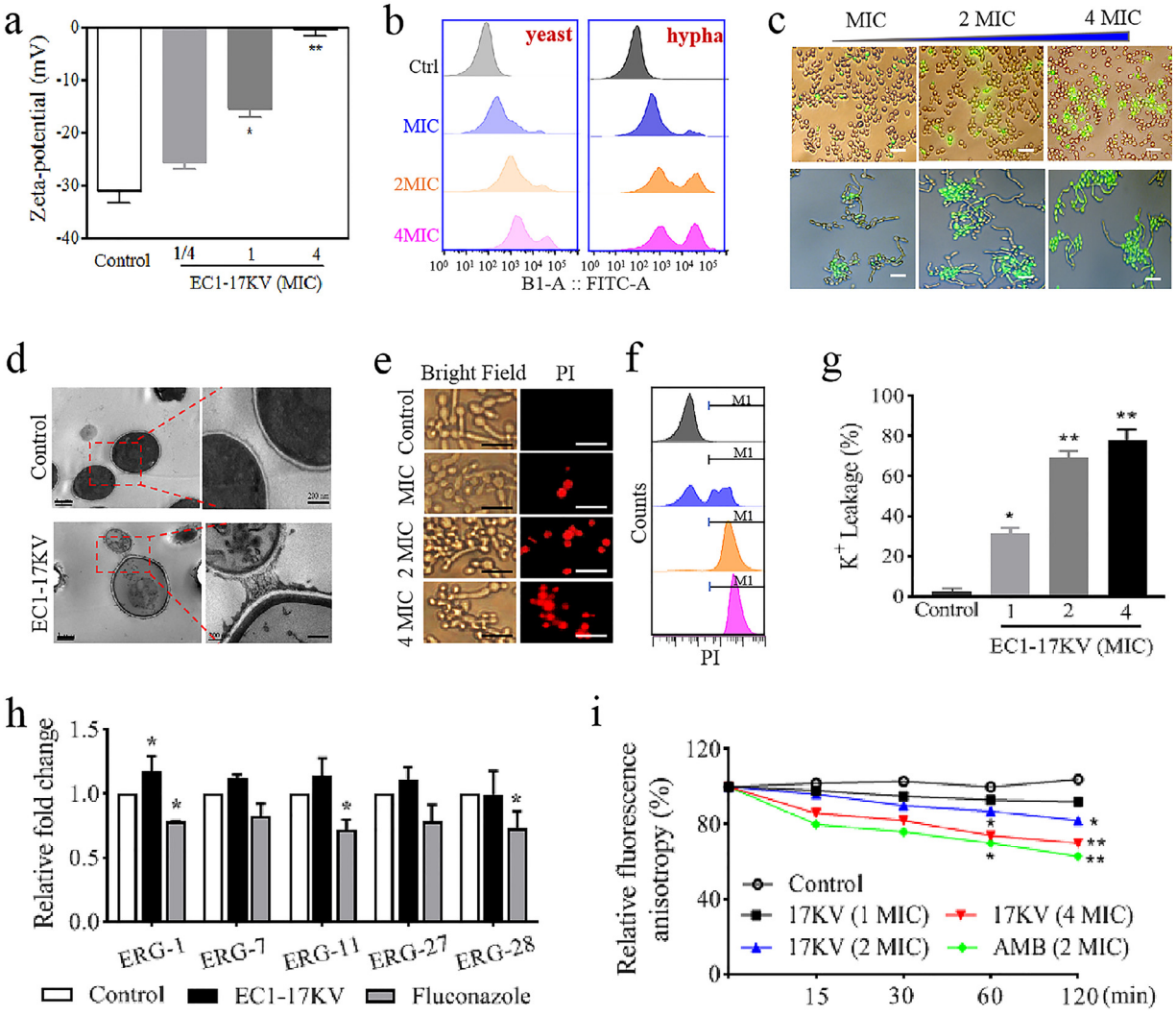

Fig. 8. EC1-17KV exerts fungicidal effects by disrupting fungal membrane integrity. (a) Zeta potential on the surface of *C. albicans*. (b) Flow cytometry and (c) fluorescence microscopy were employed to detect the binding activity of EC1-17KV to the surface of *C. albicans* (yeast and mycelial forms). Green: FITC-labelled EC1-17KV. (d) TEM assay for the ultrastructure of *C. albicans*. Images in the dotted boxes are enlarged in the rightmost column. (e-f) PI uptake and PI staining assay for the permeability of fungal cell membrane in the presence of EC1-17KV. (g) The leakage of intracellular K^+ from *C. albicans* exposed to different concentrations of EC1-17KV. (h) The expression changes of ergosterol synthesis-related genes were measured by qRT-PCR. (i) Membrane fluidity after EC1-17KV treatment was determined using a TMA-DPH probe. A decrease in DPH fluorescence anisotropy reflects an increase in membrane fluidity. Scale bars: c: 50 μm; d (left): 1 μm; d (right): 200 nm; e: 25 μm. $^*p<0.05$; $^{**}p<0.01$ *vs* control group [One-Way ANOVA Tukey test].

assay also indicated that compared with the control, EC1-17KV significantly decreased the adhesion of *C. albicans* cells, as a greater than 60% adhesion inhibition rate was achieved at peptide doses of 32 or 64 μg/ml (Fig. 9b). It has been reported that CSH is a property that exerts influence on *C. albicans* adhesion [41]. However, EC1-17KV treatment at different concentrations had no influence on CSH (Fig. 9c). This finding suggests that the reduction of *C. albicans* adherence by EC1-17KV may be attributable to factors, such as the impairment of hyphal formation and decreased recognition by phagocytic cells.

3.8.2. EC1-17KV inhibits germ tube and hypha formation

The adhered *C. albicans* on the infected surface can grow and reproduce continuously, and then further form buds and hyphae. Meanwhile, the capacity to switch between yeast, pseudohyphae and hyphae contributes to the major virulence of *C. albicans*, which is important both for tissue adhesion and invasion [42]. In this study, we observed the obvious *C. albicans* blastospore germination and germ tube formation at 1 and 2 h. However, EC1-17KV significantly inhibited the blastospore germination and germ tube formation of *C. albicans*. In addition, increasing the EC1-17KV culture time also suppressed hyphal growth in comparison with that of the vehicle control, showing markedly reduced hyphal elongation at 4 and 8 h of inoculation (Fig. 9d). Some hypha-related genes, such as HWP1, ALS3, ECE1 and EFG1, play indispensable roles in hyphal induction and growth. Here, the expression of these hypha-related genes was increased after incubation in a RPMI 1640 medium for 8 h; however, treatment with EC1-17KV significantly downregulated their expression ($p<0.05$, Fig. 9e). Data above suggest that EC1-17KV hinders the switch between yeast, pseudohyphae and hyphae by downregulating the expression of hypha-related genes.

3.8.3. EC1-17KV suppresses biofilm formation and eradicates preformed biofilms

To evaluate the antibiofilm activity of EC1-17KV, crystal violet assay for total biofilm biomass, FDA and DAPI staining for living cells, and FITC-ConA/SYPRO orange staining for EPS were respectively carried out. As shown in Fig. 9f and Fig. S4, in the absence of EC1-17KV (16 μg/ml), the seeded *C. albicans* formed a fully intact biofilm on the surfaces of cell culture plates and glass coverslips, showing a cloudy and blurred surface structure, intensive and continuous uninterrupted fluorescence, and a high OD_{595} value (total biofilm biomass).

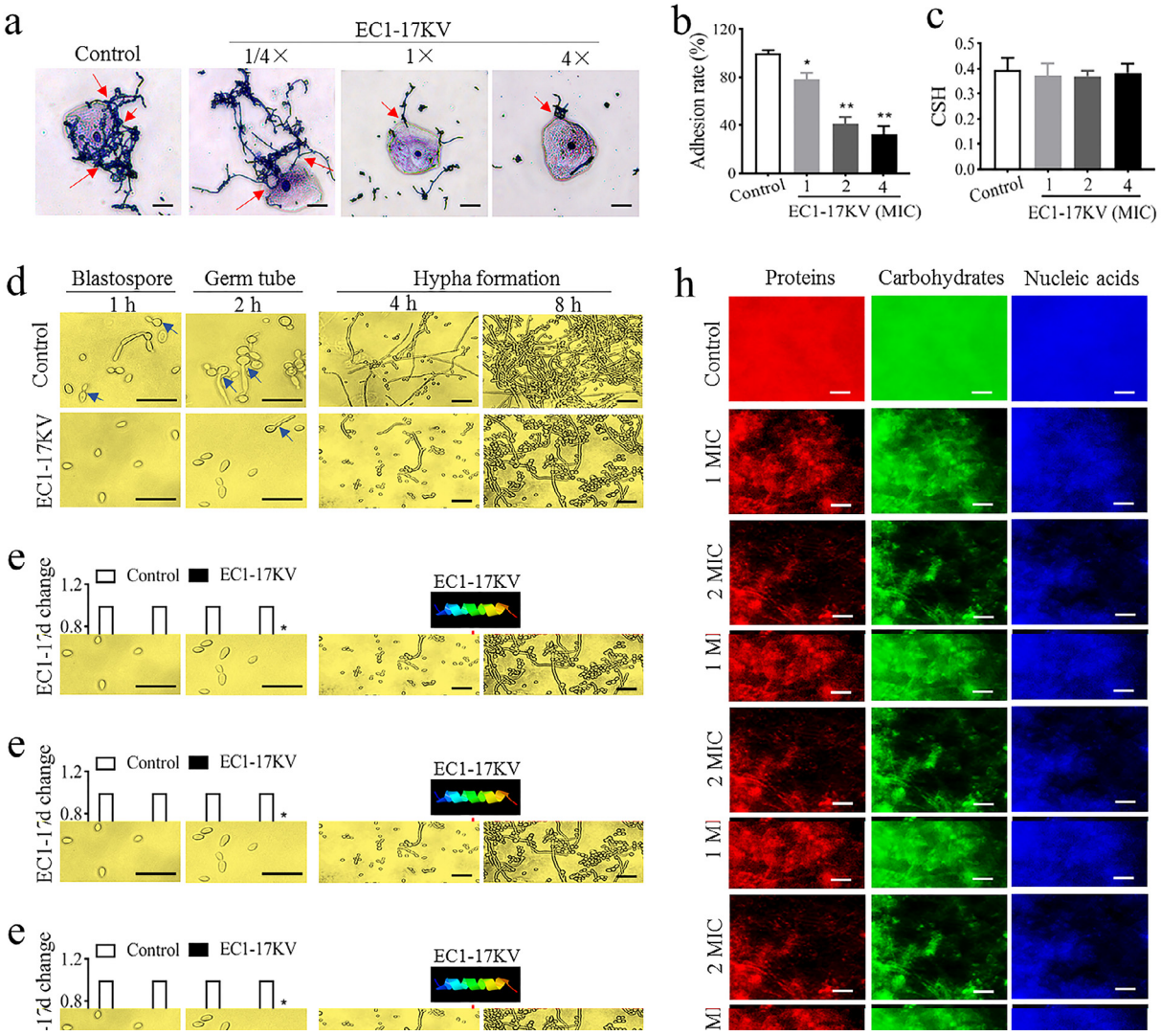

Fig. 9. EC1-17KV exerts antifungal activity by inhibiting biofilm formation and damaging preformed biofilms. The adhesion of *C. albicans* to (a) HBECs or (b) poly-L-lysine-coated polystyrene cell culture plate was detected by Wright staining or XTT assay. (c) The cell surface hydrophobicity (CSH) of EC1-17KV-treated *C. albicans* was detected. (d) Effects of EC1-17KV on hyphal formation in RPMI 1640 medium. (e) qRT-PCR analysis of the expression of filamentation-related genes (left); EC1-17KV hindered the switch between yeast, pseudohyphae and hyphae (right). The biofilm formation (f) or preformed biofilm dispersion (g) of *C. albicans* treated with EC1-17KV was detected by FDA staining and crystal violet staining. (h) EPS component reduction in preformed biofilms after EC1-17KV treatment. Carbohydrate: FITC-ConA, green; Nucleic acids: DAPI, blue; protein: SYPRO orange, red. Scale bars: a, d (right) and h: 50 μm; d (left): 25 μm; f and g: 100 μm. $^{*}p<0.05$; $^{**}p<0.01$ *vs* control group [Student *t*-test].

In contrast, EC1-17KV treatment significantly decreased both the total biofilm biomass and the fluorescence intensity of FDA (living cells), suggesting that the peptide inhibits the biofilm formation of *C. albicans*. Similarly, for preformed biofilms, EC1-17KV destroyed the integrity of the biofilms, as the fluorescence was no longer continuous and decreased by 32.7%, and some parts of the coverslip that were covered with complete biofilm became transparent. In addition, the results from crystal violet staining also confirmed that the preformed biofilms could be eradicated by the peptide, as reflected by the decreased OD_{595} value (Fig. 9g, Fig. S4). During the maturation phase of *C. albicans* biofilm development, EPS can be secreted and self-produced by *C. albicans* cells to provide protection from host immune defenses and antifungal drugs. In this study, after 72 h of culture, the fluconazole-resistant *C. albicans* secreted and produced thick and complex EPS. However, consistent with the results of the other biofilm assays, EC1-17KV markedly reduced the EPS secretion, eliminating the nucleic acids, proteins and carbohydrate components of the EPS. At 64 μg/ml (4 × MIC), the peptide reduced the EPS components by approximately 80% (Fig. 9h). This result indicates that EC1-17KV exerts inhibitory effects on EPS secretion by fluconazole-resistant *C. albicans*.

4. Discussion

To combat infections by pathogenic microbes not effectively treatable with conventional antibiotics, the de novo design of AMP based on the sequences of naturally occurring AMP is considered a promising treatment option. Although it has long been known that AMP contain positively charged and hydrophobic AA residues, the correlation of peptide sequences with biological activity has been elusive [9]. In this study, to reduce the cysteine content and shorten the sequence length to reduce the cost of synthesis, 17 AA (EC1-17) in the longer chain of EeCentrocin 1 were truncated. EC1-17 has a +5 net charge and three valines; however, this peptide displayed no antimicrobial activity against all fungi and bacteria tested. It has been reported that the balance between positively charged and hydrophobic AA residues permits cationic AMP to adopt an amphipathic conformation, which increases interaction with negatively charged surfaces and insertion into bacterial membranes [9]. Here, Asp^{8} and

Gly^{14} in the sequence of EC1-17 were replaced with Lys and Val, respectively. This modification to the mutant peptide EC1-17KV increased the α-helicity and net charge, significantly enhanced the antimicrobial activity and expanded the antimicrobial spectrum. Interestingly, after substituting Lys in the sequence of EC1-17KV to Arg (in EC1-17RV), the activity of the peptide was decreased to some extent, and the toxicity towards mammalian cells was increased, which was similar to previous reports that the incorporation of Arg residues in AMP is frequently associated with relatively higher haemolytic activities but lower antimicrobial activities compared to the use of Lys residues due to the increased α-helicity but decreased ability of self-aggregation [10, 19, 43]. The α-helicity of linear α-helical peptides is positively correlated with amphiphilicity and is closely related to antibacterial activity. EC1-17KV adopted a typical α-helical conformation in 50% SDS, 50 μM LPS or 500 μM SUVs, a hydrophobic environment (Fig. 3b-c). Importantly, it was encouraging that this lead peptide still retained its potent activity under high-salt or high-temperature conditions, differing from some AMP whose antibacterial activity might be impaired under salts at physiological concentrations [44]; this result was consistent with the reports indicated by previous studies that stability under salt conditions requires a certain proportion of cationic and hydrophobic AA [45, 46]. The above is evidence that the balance between positively charged and hydrophobic AA is a key factor controlling the activity and toxicity of AMP. Similar to some reported AMP, which induce little resistance, EC1-17KV can also circumvent drug resistance production in bacteria or fungi after 24 subcultures following the initial exposure.

Subsequently, the antimicrobial activity of EC1-17KV *in vivo* was further confirmed, showing a significant increase in animal survival rate, which may be attributed to the marked reduction of bacteria/fungi counts in mouse organs or *G. mellonella* larvae. In a murine model of systemic infection, EC1-17KV inhibited the systemic dissemination of bacteria, downregulated the expression of IL-1β/cleaved IL-1β to decrease NLRP3 inflammasome overactivation and then reduced the excessive secretion of the proinflammatory cytokines IL-1β and IL-18 and the closely associated IL-6 and TNF-α, which are important predictors for the severity of bacterial infection [32], finally alleviating inflammatory injury induced by MDR *P. aeruginosa*. In the *C. albicans*-infected *G. mellonella* model, EC1-17KV treatment resulted in complete cocoon formation and no melanin production in surviving larvae, suggesting the excellent vitality of *G. mellonella*. Notably, fluconazole displayed a poor protective effect against melanin production, histopathological injury and larval death post-infection, indicating that EC1-17KV protects *G. mellonella* against fluconazole-resistant *C. albicans* infection. Taken together, these results show that the AA substitutions made to EC1-17KV enhance the antimicrobial activity of the peptide *in vivo* and *in vitro* while eliminating its cytotoxicity towards mammalian cells, even at high concentrations.

Cationic AMP have received intense interest because of their multiple models of action for new antimicrobial therapeutics [9]. Growing evidence supports that AMP kill bacteria or fungi partly due to their direct membrane disruption activity [8, 47], whose selectivity depends on the unique membrane composition, particularly the membrane charge. The cationic charge of the peptides leads to their several-fold accumulation next to negatively charged surfaces of gram-negative bacteria or fungi, which present very different outer surfaces to attacking AMP [9]. Some AMP can quickly cross the outer membrane presented by gram-negative bacteria, which is negatively charged due to the existence of LPS, by a charge-exchange mechanism where the cationic peptides compete with Ca^{2+} and Mg^{2+} bound to LPS [9]. Similarly, EC1-17KV induced an obvious release of Ca^{2+} and LPS into the supernatant, and the addition of external Ca^{2+} ($\geq$1.0 mM) reduced the EC1-17KV-induced LPS release and drastically enhanced the MIC values of EC1-17KV against *P. aeruginosa*. Interestingly, after the chelation of external Ca^{2} by EDTA, the MIC fold changes were obviously decreased, indicating that this peptide may competitively replace Ca^{2+} to bind to LPS, resulting in the destruction of bacterial membrane integrity. In fungal membranes, glycerophospholipids generally present a more negative fungal membrane due to the higher phosphatidylinositol and phosphatidic acid versus the predominantly neutral mammalian host cell membranes with high phosphatidylcholine [38]. As demonstrated in our study, the *C. albicans* surface was negatively charged (-31.1 mV), and EC1-17KV dose-dependently neutralized the negative charge; after 30 min of coincubation, aggregated on the surface of *Candida* in both yeast and mycelial forms. The membrane fluidity of fungi is a key factor affecting the activity of antifungal drugs. Ergosterol, as a typical plasma membrane component, plays a critical role in membrane fluidity; hence, disruption of its synthesis has become a focus of antifungal therapies. However, EC1-17KV could not inhibit but slightly promoted the expression of ergosterol synthesis-related genes, which needs to be clarified in future studies. Interestingly, the relative fluorescence intensity of TMA-DPH, a hydrophobic molecule probe that potentially interacts with the phospholipid portion of the plasma membrane without compromising the overall lipid bilayer structure [39], decreased as the peptide concentration increased, suggesting high membrane fluidity. This indicates that the accumulated EC1-17KV may subsequently insert into the lipid bilayer of the *C. albicans* cell membrane. This membrane-destruction effect of AMP leads to noticeable disruption of the plasma membrane, nuclear structure and intracellular organelles; leakage of intracellular contents; and even the loss of bacterial structure, ultimately killing bacteria or fungi. We consistently observed that EC1-17KV ($\geq 2 \times$ MIC) caused significant membrane destruction in both planktonic *C. albicans* and *P. aeruginosa* according to the results from the NPN/PI uptake tests, SYTO9/PI staining, liposome-loaded calcein release and intracellular K^+ release assays, and TEM detection. Consequently, EC1-17KV powerfully killed drug-resistant bacteria or fungi.

Biofilm-related infections always result in increased patient mortality and drug resistance [2]. Planktonic *P. aeruginosa* and *C. albicans* are capable of colonizing the surfaces of various prosthetic materials, forming biofilms that hinder the action of antibiotics that can lead to serious infections, such as catheter-associated urinary tract infection [48]. We found that EC1-17KV inhibited biofilm formation and dispersed the mature biofilm of MDR *P. aeruginosa* and fluconazole-resistant *C. albicans*. In addition, EC1-17KV also exhibited excellent biofilm eradication activity in mice implanted with a biofilm-containing catheter. That is, EC1-17KV reduced the number of sessile *P. aeruginosa* attached to the catheter surface and inhibited the diffusion of bacteria from the catheter into the subcutaneous tissue to improve tissue injury. Increasing evidence has proven that several Trp/Arg-containing AMP are able to kill persister cells [49, 50]; thus, the direct targeting of the cell membrane by EC1-17KV may contribute to its high level of effectiveness against these dormant persister cells and potent antibiofilm activity. The adherence of *C. albicans* to host cells or abiotic surfaces is the first step in the biofilm formation process. In the present study, EC1-17KV reduced *C. albicans* adherence to HBECs or poly-L-lysine-coated polystyrene cell culture plates and glass. After adhering to a surface, *C. albicans* can grow and reproduce continuously and further form buds, hyphae and biofilms. Importantly, EC1-17KV also decreased blastospore germination and germ tube formation because it downregulated the expression of the hypha-related genes *HWP1*, *ALS3*, *ECE1* and *EFG1*, which encodes adhesin proteins, regulates adhesion function and cell elongation, or regulates hyphae formation.

5. Conclusion

To develop a new type of weapon in the arms race against bacteria, we generated three synthetic peptides based on the *Echinus esculentus* antimicrobial peptide EeCentrocin 1. The lead candidate, EC1-

17KV, can kill MDR *P. aeruginosa* and fluconazole-resistant *C. albicans* in many contexts, including in systemically infected mice/*G. mellonella* larvae and in local biofilm-implanted mice, without producing particularly noteworthy toxicity to mammalian cells at MBCs/MFCs. Long-term exposure to EC1-17KV did not induce bacterial or fungal resistance. High-salt levels and high temperature did not affect the structure and activity of EC1-17KV. It has multiple modes of action, including direct membrane disruption and inhibitory effects on cell adhesion, hyphal formation and biofilm formation. Topical application of EC1-17KV could one day be used in biomedical coatings and healthcare formulas to help patients combat bacteria or fungi that are resistant to traditional antibiotics.

Research in context

Evidence before this study

Biofilm-associated infections induced by multidrug-resistant strains are largely responsible for untreatable infections. The therapeutic approach of multidrug-resistant *P. aeruginosa* and *C. albicans* is still controversial. EeCentrocin 1 with long amino acid sequence and cysteine content increases the cost and difficulty of synthesis. Furthermore, EeCentrocin 1 and 2, EeStrongylocin 2 and Ee4635, and the longer chain of EeCentrocin 1 all had a relatively poor antifungal activity and antimicrobial spectrum.

Added value of this study

Designed cationic peptide EC1-17KV, derived from *Echinus esculentus*, had short amino acid sequence, low toxicity and broad antimicrobial spectrum against various drug-resistant bacteria and fungi *in vivo/vitro*. Long-term exposure to EC1-17KV did not induce bacterial or fungal resistance. High salt/temperature did not affect the activity of EC1-17KV. Its multiple modes of action involve in membrane disruption and antibiofilm effects.

Implications of all the available evidence

Multidrug resistant strains are rising. For infections induced by multidrug-resistant *P. aeruginosa* or *C. albicans*, EC1-17KV may be a potential candidate for use in biomedical coatings and healthcare formulas due to its multiple mechanisms, low toxicity and high efficacy.

Funding sources

This work was funded by the National Natural Science Foundation of China (No. 81673483, 81803591); National Science and Technology Major Project Foundation of China (2019ZX09721001-004-005); National Key Research and Development Program of China (2018YFA0902000); "Double First-Class" University project (CPU2018GF/GY16); Young Scientists of Natural Science Foundation of Jiangsu Province of China (No. BK20180563); and a Project Funded by the Priority Academic Program Development (PAPD) of Jiangsu Higher Education Institutions. The sponsors of the study had not any role in study design, data collection, data analysis, interpretation, and writing of the report.

Authorship contribution statement

ML and ZC designed research; ML, YX, SP, XP, WL, LZ, HX and BZ performed the experiments; ML, YX, SP, BZ analyzed the data and finished the figures; ML and BZ wrote the manuscript. ML and ZC reviewed and edited the manuscript. All authors read and approved the manuscript.

Declaration of Competing Interest

The authors declare that they have no conflicts of interest.

Supplementary materials

Supplementary material associated with this article can be found, in the online version, at doi:10.1016/j.ebiom.2020.102775.

References

[1] Frieri M, Kumar K, Boutin A. Antibiotic resistance. J Infect Public Health 2017;10:369–78.
[2] Hall CW, Mah TF. Molecular mechanisms of biofilm-based antibiotic resistance and tolerance in pathogenic bacteria. FEMS Microbiol Rev 2017;41:276–301.
[3] Maraolo AE, Cascella M, Corcione S, Cuomo A, Nappa S, Borgia G, et al. Management of multidrug-resistant Pseudomonas aeruginosa in the intensive care unit: state of the art. Expert Rev Anti Infect Ther 2017;15:861–71.
[4] Zhang JY, Liu JH, Liu FD, Xia YH, Wang J, Liu X, et al. Vulvovaginal candidiasis: species distribution, fluconazole resistance and drug efflux pump gene overexpression. Mycoses 2014;57:584–91.
[5] Break TJ, Desai JV, Natarajan M, Ferre EMN, Henderson C, Zelazny AM, et al. VT-1161 protects mice against oropharyngeal candidiasis caused by fluconazole-susceptible and -resistant Candida albicans. J Antimicrob Chemother 2018;73:151–5.
[6] Lee H, Lim SI, Shin SH, Lim Y, Koh JW, Yang S. Conjugation of Cell-Penetrating Peptides to Antimicrobial Peptides Enhances Antibacterial Activity. ACS Omega 2019;4:15694–701.
[7] Sanchez-Gomez S, Martinez-de-Tejada G. Antimicrobial Peptides as Anti-biofilm Agents in Medical Implants. Curr Top Med Chem 2017;17:590–603.
[8] Ma L, Wang Y, Wang M, Tian Y, Kang W, Liu H, et al. Effective antimicrobial activity of Cbf-14, derived from a cathelin-like domain, against penicillin-resistant bacteria. Biomaterials 2016;87:32–45.
[9] Bechinger B, Peptides Gorr SUAntimicrobial. Mechanisms of Action and Resistance. J Dent Res 2017;96:254–60.
[10] Ong ZY, Wiradharma N, Yang YY. Strategies employed in the design and optimization of synthetic antimicrobial peptide amphiphiles with enhanced therapeutic potentials. Adv Drug Deliv Rev 2014;78:28–45.
[11] Solstad RG, Li C, Isaksson J, Johansen J, Svenson J, Stensvag K, et al. Novel Antimicrobial Peptides EeCentrocins 1, 2 and EeStrongylocin 2 from the Edible Sea Urchin Echinus esculentus Have 6-Br-Trp Post-Translational Modifications. PLoS One 2016;11:e0151820.
[12] Solstad RG, Johansen C, Stensvag K, Strom MB, Haug T. Structure-activity relationship studies of shortened analogues of the antimicrobial peptide EeCentrocin 1 from the sea urchin Echinus esculentus. J Pept Sci 2020;26:e3233.
[13] Subbalakshmi C, Nagaraj R, Sitaram N. Biological activities of C-terminal 15-residue synthetic fragment of melittin: design of an analog with improved antibacterial activity. Febs Lett 1999;448:62–6.
[14] Park Y, Park SC, Park HK, Shin SY, Kim Y, Hahm KS. Structure-activity relationship of HP (2-20) analog peptide: enhanced antimicrobial activity by N-terminal random coil region deletion. Biopolymers 2007;88:199–207.
[15] Monteiro C, Pinheiro M, Fernandes M, Maia S, Seabra CL, Ferreira-da-Silva F, et al. A 17-mer Membrane-Active MSI-78 Derivative with Improved Selectivity toward Bacterial Cells. Mol Pharm 2015;12:2904–11.
[16] Chan DI, Prenner EJ, Vogel HJ. Tryptophan- and arginine-rich antimicrobial peptides: structures and mechanisms of action. Biochim Biophys Acta 2006;1758:1184–202.
[17] Torres MDT, Sothiselvam S, Lu TK, de la Fuente-Nunez C. Peptide Design Principles for Antimicrobial Applications. J Mol Biol 2019;431:3547–67.
[18] Drin G, Antonny B. Cell biology: helices sculpt membrane. Nature 2005;437:1247–9.
[19] Wiradharma N, Khoe U, Hauser CA, Seow SV, Zhang S, Yang YY. Synthetic cationic amphiphilic alpha-helical peptides as antimicrobial agents. Biomaterials 2011;32:2204–12.
[20] Yang AS, Honig B. Free energy determinants of secondary structure formation: I. alpha-Helices. J Mol Biol 1995;252:351–65.
[21] Sani MA, Saenger C, Juretic D, Separovic F. Glycine Substitution Reduces Antimicrobial Activity and Helical Stretch of diPGLa-H in Lipid Micelles. J Phys Chem B 2017;121:4817–22.
[22] Saint Jean KD, Henderson KD, Chrom CL, Abiuso LE, Renn LM, Caputo GA. Effects of Hydrophobic Amino Acid Substitutions on Antimicrobial Peptide Behavior. Probiotics Antimicrob Proteins 2018;10:408–19.
[23] Yu C, Wei S, Han X, Liu H, Wang M, Jiang M, et al. Effective inhibition of Cbf-14 against Cryptococcus neoformans infection in mice and its related anti-inflammatory activity. Fungal Genet Biol 2018;110:38–47.
[24] Zgoda JR, Porter JR. A convenient microdilution method for screening natural products against bacteria and fungi. Pharm Biol 2001;39:221–5.
[25] Ji S, Li W, Zhang L, Zhang Y, Cao B. Cecropin A-melittin mutant with improved proteolytic stability and enhanced antimicrobial activity against bacteria and fungi associated with gastroenteritis in vitro. Biochem Biophys Res Commun 2014;451:650–5.
[26] Gao T, Zeng H, Xu H, Gao F, Li W, Zhang S, et al. Novel Self-assembled Organic Nanoprobe for Molecular Imaging and Treatment of Gram-positive Bacterial Infection. Theranostics 2018;8:1911–22.
[27] Scorzoni L, de Lucas MP, Mesa-Arango AC, Fusco-Almeida AM, Lozano E, Cuenca-Estrella M, et al. Antifungal efficacy during Candida krusei infection in non-conventional models correlates with the yeast in vitro susceptibility profile. PLoS One 2013;8:e60047.

[28] Sun Y, Dong WB, Sun L, Ma LJ, Shang DJ. Insights into the membrane interaction mechanism and antibacterial properties of chensinin-1b. Biomaterials 2015;37:299–311.
[29] Souza L, Silva-Rocha WP, Ferreira MRA, Soares LAL, Svidzinski TIE, Milan EP, et al. Influence of Eugenia uniflora Extract on Adhesion to Human Buccal Epithelial Cells, Biofilm Formation, and Cell Surface Hydrophobicity of Candida spp. from the Oral Cavity of Kidney Transplant Recipients. Molecules 2018:23.
[30] Han Y, Zhao J, Zhang B, Shen Q, Shang Q, Li P. Effect of a novel antifungal peptide P852 on cell morphology and membrane permeability of Fusarium oxysporum. Biochim Biophys Acta Biomembr 2019;1861:532–9.
[31] Travis SM, Anderson NN, Forsyth WR, Espiritu C, Conway BD, Greenberg EP, et al. Bactericidal activity of mammalian cathelicidin-derived peptides. Infect Immun 2000;68:2748–55.
[32] Pierrakos C, Vincent JL. Sepsis biomarkers: a review. Crit Care 2010;14:R15.
[33] Rajasekaran G, Kumar SD, Yang S, Shin SY. The design of a cell-selective fowlicidin-1-derived peptide with both antimicrobial and anti-inflammatory activities. Eur J Med Chem 2019;182:111623.
[34] Lee JK, Park SC, Hahm KS, Park Y. A helix-PXXP-helix peptide with antibacterial activity without cytotoxicity against MDRPA-infected mice. Biomaterials 2014;35:1025–39.
[35] Dinarello CA. Interleukin-1 in the pathogenesis and treatment of inflammatory diseases. Blood 2011;117:3720–32.
[36] Kovarova M, Hesker PR, Jania L, Nguyen M, Snouwaert JN, Xiang Z, et al. NLRP1-dependent pyroptosis leads to acute lung injury and morbidity in mice. J Immunol 2012;189:2006–16.
[37] Clifton LA, Skoda MW, Le Brun AP, Ciesielski F, Kuzmenko I, Holt SA, et al. Effect of divalent cation removal on the structure of gram-negative bacterial outer membrane models. Langmuir 2015;31:404–12.
[38] Rautenbach M, Troskie AM, Vosloo JA. Antifungal peptides: To be or not to be membrane active. Biochimie 2016;130:132–45.
[39] Choi H, Cho J, Jin Q, Woo ER, Lee DG. Antifungal property of dihydrodehydrodiconiferyl alcohol 9′-O-beta-D-glucoside and its pore-forming action in plasma membrane of Candida albicans. Biochim Biophys Acta 2012;1818:1648–55.
[40] Southern P, Horbul J, Maher D, Davis DA. C. albicans colonization of human mucosal surfaces. PLoS One 2008;3:e2067.
[41] Araujo D, Henriques M, Silva S. Portrait of Candida Species Biofilm Regulatory Network Genes. Trends Microbiol 2017;25:62–75.
[42] Noble SM, Gianetti BA, Witchley JN. Candida albicans cell-type switching and functional plasticity in the mammalian host. Nat Rev Microbiol 2017;15:96–108.
[43] Irazazabal LN, Porto WF, Ribeiro SM, Casale S, Humblot V, Ladram A, et al. Selective amino acid substitution reduces cytotoxicity of the antimicrobial peptide mastoparan. Biochim Biophys Acta 2016;1858:2699–708.
[44] Tripathi AK, Kumari T, Tandon A, Sayeed M, Afshan T, Kathuria M, et al. Selective phenylalanine to proline substitution for improved antimicrobial and anticancer activities of peptides designed on phenylalanine heptad repeat. Acta Biomater 2017;57:170–86.
[45] Yu HY, Tu CH, Yip BS, Chen HL, Cheng HT, Huang KC, et al. Easy strategy to increase salt resistance of antimicrobial peptides. Antimicrob Agents Chemother 2011;55:4918–21.
[46] Tan P, Lai Z, Jian Q, Shao C, Zhu Y, Li G, et al. Design of Heptad Repeat Amphiphiles Based on Database Filtering and Structure-Function Relationships to Combat Drug-Resistant Fungi and Biofilms. ACS Appl Mater Interfaces 2020;12:2129–44.
[47] Ma L, Xie X, Liu H, Huang Y, Wu H, Jiang M, et al. Potent antibacterial activity of MSI-1 derived from the magainin 2 peptide against drug-resistant bacteria. Theranostics 2020;10:1373–90.
[48] Raman N, Lee MR, Rodriguez Lopez AL, Palecek SP, Lynn DM. Antifungal activity of a beta-peptide in synthetic urine media: Toward materials-based approaches to reducing catheter-associated urinary tract fungal infections. Acta Biomater 2016;43:240–50.
[49] de Breij A, Riool M, Cordfunke RA, Malanovic N, de Boer L, Koning RI, et al. The antimicrobial peptide SAAP-148 combats drug-resistant bacteria and biofilms. Sci Transl Med 2018:10.
[50] Chen X, Zhang M, Zhou C, Kallenbach NR, Ren D. Control of bacterial persister cells by Trp/Arg-containing antimicrobial peptides. Appl Environ Microbiol 2011;77:4878–85.